



Benchmark problems for nonlinear system identification and control using Soft Computing methods: Need and overview



Andreas Kroll^{a,*}, Horst Schulte^b

^a University of Kassel, Measurement and Control Department, Mechanical Engineering Faculty, Germany

^b HTW University of Applied Science Berlin, Department of Engineering I, Control Engineering, Germany

ARTICLE INFO

Article history:

Received 6 September 2013

Received in revised form 9 July 2014

Accepted 14 August 2014

Available online 6 September 2014

Keywords:

Benchmarking

Nonlinear control

Nonlinear system identification

ABSTRACT

Using benchmark problems to demonstrate and compare novel methods to the work of others could be more widely adopted by the Soft Computing community. This article contains a collection of several benchmark problems in nonlinear control and system identification, which are presented in a standardized format. Each problem is augmented by examples where it has been adopted for comparison. The selected examples range from component to plant level problems and originate mainly from the areas of mechatronics/drives and process systems. The authors hope that this overview contributes to a better adoption of benchmarking in method development, test and demonstration.

© 2014 Elsevier B.V. All rights reserved.

1. Introduction

Once new Soft Computing (SC) methods are developed, it is of key interest to compare their performance in relation to state-of-the-art methods in order to position them. However, such comparisons seldom take place due to the efforts of adopting sufficient insight in and control over methods other than the own research focus. This problem can be circumvented if benchmark problems are adopted more widely such that one can retrieve competing results from literature without having to master other methods. In fact, well-established benchmark problems are available for problems such as classification, control and modeling, to name a few. The objective of this article is to present selected (nonlinear) benchmark problems for identification and control, and to promote a wider adoption to provide a framework for comparing alternative SC methods. A word of caution is due: Methods typically work better on some and worse on other problems. Hence, good results on a single benchmark problem highlight advantages for respective problem types but should not be generalized.

Benchmarking is based on the principles of the ability to be validated, reproducibility and comparability. This requires exact specification of benchmark problems spanning from the process description over experiment design, test data to assessment criteria

for obtained results. Unfortunately, even complete and commonly adopted “benchmark” problems often do not provide a complete, self-enclosed description. A typical situation is that a process model to be used is described well; however engineering details, experiment/test design and assessment criteria are incomplete or lacking.

In the following section, sets of assessment criteria are proposed for modeling and control. Section 3 contains the benchmark problems. The presented selection does not attempt to be complete but rather offer attractive problems for the Soft Computing community. The sequence was designed to start from simple component and ascend to plant level problems. This article is an extended version of the identification and control part of a position paper written for the German GMA technical committee on Computational Intelligence [33].

2. Assessment criteria

2.1. Model performance

Criteria to assess the results of modeling tasks can address approximation quality, model complexity and model interpretability [47]. Most commonly, the approximation/prediction error is used as assessment criterion. Most significant is the result for validation/test rather than for the training data. Many different criteria are proposed as e.g. sometimes the worst case and sometimes the average deviation may be more important. In case of benchmark problems, it is recommended to report a few widely accepted criteria such as a subset of the following ones: Given N data sets where

* Corresponding author. Tel.: +49 5618043248.

E-mail addresses: andreas.kroll@mrt.uni-kassel.de (A. Kroll), horst.schulte@htw-berlin.de (H. Schulte).

$y(k)$ is the output of a system and $\hat{y}(k)$ the corresponding output of the model, this could be the *maximum absolute error* (MAE)

$$J_{MAE} = J_{\max} = \max_{1 \leq k \leq N} |y(k) - \hat{y}(k)|, \quad (1)$$

the *sum of squared errors* (SSE)

$$J_{SSE} = \sum_{k=1}^N (y(k) - \hat{y}(k))^2, \quad (2)$$

the *mean squared error* (MSE)

$$J_{MSE} = \frac{1}{N} \sum_{k=1}^N (y(k) - \hat{y}(k))^2, \quad (3)$$

and/or the *root mean squared error* (RMSE)

$$J_{RMSE} = \sqrt{J_{MSE}}. \quad (4)$$

The measure *variance accounting for* (VAF)

$$J_{VAF} = \left(1 - \frac{\text{Var}(y(k) - \hat{y}(k))}{\text{Var}(y(k))} \right) \cdot 100\%, \quad (5)$$

origins from linear regression where it provides the percentage of the variance of y that can be explained by the used linear regression model.¹ $\text{Var}(\circ)$ gives the variance of \circ . J_{VAF} can be estimated by the coefficient of determination R^2

$$R^2 = 1 - \frac{\sum_{k=1}^N (y(k) - \hat{y}(k))^2}{\sum_{k=1}^N (y(k) - \bar{y})^2} \quad \text{with} \quad \bar{y} = \frac{1}{N} \sum_{k=1}^N y(k). \quad (6)$$

To admit comparing models with different numbers of parameters R^2 is adjusted to

$$R_a^2 = 1 - \frac{N-1}{N - (\dim(\Theta) + 1)} \cdot (1 - R^2). \quad (7)$$

A related measure is the *normalized mean squared error* (NMSE)

$$J_{NMSE} = \frac{\sum_{k=1}^N (y(k) - \hat{y}(k))^2}{\sum_{k=1}^N (y(k) - \bar{y})^2}, \quad (8)$$

and the *best fit rate* (BFR)

$$J_{BFR} = \left(1 - \frac{\sqrt{\sum_{k=1}^N (y(k) - \hat{y}(k))^2}}{\sqrt{\sum_{k=1}^N (y(k) - \bar{y})^2}} \right) \cdot 100\% \quad (9)$$

Note, that J_{VAF} and J_{BFR} can take negative value, which are typically replaced by 0. k is the discrete time with $t = k T_0$, T_0 : sampling time. Common practice is to additionally assess the frequency distribution of the residual $\epsilon(k) = y(k) - \hat{y}(k)$ wrt. to mean, shape and symmetry of the tails. This provides a qualitative indication whether the residuals are normally distributed.

It is important to differentiate between one-step-ahead and recursive model evaluation: In the first case measurements available until present time k are used to predict the output $\hat{y}(k+1)$ one-step-ahead into the future

$$\hat{y}(k+1) = f(y(k), \dots, y(k-n), \mathbf{u}(k-\tau), \dots, \mathbf{u}(k-\tau-m)), \quad (10)$$

where n and m , respectively, is the number of lagged terms considered and τ a discrete dead-time. In a second case, lagged predictions are used as model inputs instead of measured data:

$$\hat{y}(k+1) = f(\hat{y}(k), \dots, \hat{y}(k-n), \mathbf{u}(k-\tau), \dots, \mathbf{u}(k-\tau-m)). \quad (11)$$

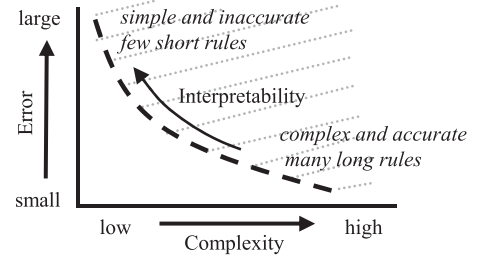


Fig. 1. Illustration of a typical relationship between approximation quality, complexity and interpretability of a model [47].

Good recursive model evaluation results are more difficult to achieve than good one-step-ahead predictions. In case models of different complexity yield similar approximation performance, the simpler model should be preferred (“Ockham’s principle”). Model-complexity-oriented criteria take this into account by valuing the number of parameters (as a measure for model complexity) besides the approximation error. An example of such a criterion is Akaike’s Final Prediction Error (FPE)

$$J_{FPE} = \frac{1 + \dim(\Theta)/N}{1 - \dim(\Theta)/N} \cdot \frac{1}{N} \sum_{k=1}^N (\hat{y}(k, \Theta) - y(k))^2. \quad (12)$$

In case of multi-input multi-output systems above recorded, criteria can be assessed individually for the outputs. Alternatively, the quantities can be scaled and aggregated to a single metric as in Section 3.9.

Other criteria are recorded e.g. in [61]. Ease of model interpretability is a meaningful concept for comparing fuzzy and neuro-fuzzy rule-based models, see Fig. 1. However, interpretability is difficult to define as a metric criterion.

2.2. Control performance

Criteria to assess the control performance include the step response, reference tracking, disturbance rejection behavior and the control effort. This is analyzed for the nominal case and in some benchmark problems also with predefined structured model uncertainties. The latter is application-dependent. However, the general procedure is discussed in this section. Therefore, details will be given in relation to the individual benchmarks.

As previously described for the modeling task, widely accepted criteria and related measures will be analogously given in the following: The *step response* is used to characterize the accuracy, damping and speed of the closed loop system. To measure the steady state accuracy the integrated absolute error (IAE) is given by

$$J_{IAE} = \sum_{k=1}^N |y(k) - y_{ss}| T_0 \quad (13)$$

with y_{ss} as the steady-state response. Common practice is to measure the maximum percent overshoot (PO)

$$J_{PO} = \frac{\max_{1 \leq k \leq N} (y(k) - y_{ss})}{y_{ss}} \cdot 100\% \quad (14)$$

and maximum percent undershoot (PU)

$$J_{PU} = \frac{\max_{1 \leq k \leq N} (-y(k))}{y_{ss}} \cdot 100\%. \quad (15)$$

The *reference tracking criteria* are concerned with the response of the closed-loop system to the time-variable reference $r(t)$ alone,

¹ Note, that it loses the original statistical interpretation when applied to nonlinear models.

disregarding the effect of disturbance on the process. The tracking response can be defined as

$$y_r(t) = T(\Theta_c, r(t)), \quad (16)$$

where Θ_c denotes the controller parameter vector. A fundamental objective of a control system is to make the process output y_r as close as possible to the reference. The control performance can be evaluated by the *maximum absolute tracking error* (MAE)

$$J_{MAE_{Ref}} = J_{max} = \max_{1 \leq k \leq N} |r(k) - y_r(k)|, \quad (17)$$

the mean squared tracking error

$$J_{MSE_{Ref}} = \frac{1}{N} \sum_{k=1}^N (r(k) - y_r(k))^2 \quad \text{with } t = k \cdot T_0, \quad (18)$$

and the root mean squared tracking error

$$J_{RMSE_{Ref}} = \sqrt{J_{MSE_{Ref}}}. \quad (19)$$

As previously described in Section 2.1 the normalized mean squared tracking error (NMSE) is

$$J_{NMSE_{Ref}} = \frac{\sum_{k=1}^N (r(k) - y_r(k))^2}{\sum_{k=1}^N (r(k) - \bar{r})^2}, \quad (20)$$

For the special case of a fixed set point r_{sp} the related measure is

$$J_{NMSE_{Sp}} = \frac{\sum_{k=1}^N (r_{sp} - y_r(k))^2}{\sum_{k=1}^N r_{sp}^2}. \quad (21)$$

It must be emphasized that it is usually impossible to obtain perfect tracking. No matter how good the design is, no controller can make the output to exactly track the reference. That is, the performance criterion (18) and (19) can never be made zero. Since perfect tracking is not possible, the tracking objective is usually relaxed into a specification of how close a tracking would be satisfactory for the designer.

Control effort: Most actuators (electric motors, an aircraft rudder, a combustion engine) have only a fixed output range. To account for this the control effort can be measured by the peak control effort

$$J_{peak_u} = \max_{1 \leq k \leq N} |u(k)| \quad (22)$$

with the manipulated variable u , the integral squared control action

$$J_{ISU} = \sum_{k=1}^N (u(k) - \bar{u})^2, \quad \bar{u} = \frac{1}{N} \sum_{k=1}^N u(k) \quad (23)$$

and the maximum overshoot of the manipulated variable

$$J_{OS_u} = \max_{1 \leq k \leq N} |u(k) - u_{ss}|. \quad (24)$$

Disturbance rejection criteria: Another fundamental control objective is to minimize the effect of the disturbance on the controlled output. The output of the closed-loop system due to the disturbance, disregarding the effect of the reference, is given by

$$y_z(t) = S(\Theta_c, d(t)), \quad (25)$$

where d denotes the disturbance signal. To verify the disturbance rejection performance different types of deterministic and stochastic disturbances are used:

1. The deterministic disturbance can be approximated by a series of step signals:

$$d(t) = d_1(t) + d_2(t) + \dots + d_n(t) \quad (26)$$

where

$$d_i(t) = \begin{cases} 0 & , \quad 0 \leq t \leq t_i \\ D_i & , \quad t \geq t_i \end{cases} \quad (27)$$

which can be optionally extended by ramp-shaped disturbances.

2. Stochastic disturbances can be characterized simply by Gaussian random variables with the expected value $E\{d(t)\} = 0$ and $\text{var}\{d(t)\} = \sigma^2$.

The effect of the disturbance on the output can be measured by the mean squared error around a fixed operating point y_{sp}

$$J_{MSE_{Dst}} = \frac{1}{N} \sum_{k=1}^N (y_z(k) - y_0(k))^2, \quad (28)$$

and the root mean squared error

$$J_{RMSE_{Dst}} = \sqrt{J_{MSE_{Dst}}}. \quad (29)$$

Again, it is clear that no controller can make the effect of the disturbance to disappear completely, that is, to make (28) and (29) become zero. Also in this case, the quantified specification is given by the upper bound of (28) and (29).

Robustness: Control systems are designed based on reduced models of the processes where the dynamics will often change during operation. The sensitivity of the performance of closed loop system to variations in process dynamics is therefore a fundamental issue. To describe the process changes during operation a sufficient percentage deviation from nominal parameter values are considered. The interval width is application dependent and can vary over a wide range of capacity of the nominal value Θ_{c0} . For example, if it is known that the work load of a robot manipulator can vary from 15% to 120% of capacity, then the controller are robust to varying loads if it can tolerate variations within this range without unacceptable deviation from nominal performance.

3. Benchmark problems

3.1. Artificial system identification problems

Motivation: Identification problems can be created artificially by specifying a nonlinear dynamic model (without any physical interpretation), which is used to generate data for system identification. In particular, several single-input single-output (SISO) systems have been defined this way, as they are quick first test problems. Some examples have been adopted several times and recognized as benchmark problems. Two such examples will be presented in the following.

Process description: Five problems are specified in [60]. One of which ("example 2") is the second-order difference equation

$$y(k+1) = \frac{y(k)}{1+y^2(k)} \frac{y(k-1)}{y^2(k-1)} + 2.5 + u(k) \quad (30)$$

of a single-input single-output (SISO) system. A signal composed of 10^5 realizations of an i.i.d.² random variable $u(k)$, that is uniformly distributed in $[-2; 2]$, is used for identification. For validation, $u(k) = \sin(2\pi k/25)$ is proposed.

² independent and identically distributed.

Table 1
Data sets available in *DalSy* [15].

Ethane-ethylene distillation column	Laboratory setup acting like a hair dryer
Glass furnace	CD-player arm
120 MW power plant	Wing flutter data
Industrial evaporator	Flexible robot arm
pH-neutralization process in a stirring tank	Steel-subframe-flexible structure
Fractional distillation column	Cutaneous potential recordings of a pregnant woman
Industrial dryer	Tongue displacement shapes occurring in the pronunciation of English vowels by different English-speaking persons
Liquid-saturated steam heat exchanger	Western basin of Lake Erie
Industrial winding process	Heat flow density through a two layer wall
Continuously stirred tank reactor	Heating system
Steam generator at Abbott Power Plant	Simulator of in-vivo MRS-signals
Ball-and-beam setup in SISTA	One hour of Internet traffic between the Lawrence Berkeley Laboratory and the rest of the world

A second example (“example 4”) is the following two-input two-output system:

$$\begin{bmatrix} y_1(k+1) \\ y_2(k+1) \end{bmatrix} = \begin{bmatrix} \frac{y_1(k)}{1+y_2^2(k)} \\ \frac{y_1(k)}{1+y_2^2(k)} \end{bmatrix} + \begin{bmatrix} u_1(k) \\ u_2(k) \end{bmatrix}. \quad (31)$$

10^5 realizations of i.i.d. random variables $u_1(k)$ and $u_2(k)$, respectively, which are uniformly distributed in $[-1;1]$, are used for identification. For validation, $u_1(k) = \sin(2\pi k/25)$ and $u_2(k) = \cos(2\pi k/25)$ are proposed.

Problem description: The process description can be used to test and demonstrate nonlinear system identification methods in a “clinical environment”. In [60], series-parallel models are identified.

Assessment criteria: A “suitable” norm of the prediction error observed in one-step-ahead model evaluation is proposed as criterion.

Examples of reported use: In [82], an algorithm to identify multivariable discrete-time dynamic Takagi-Sugeno systems in a noisy environment is introduced and tested on both benchmark problems. However, different test signals are used in the SISO case. J_{MSE} and J_{VAF} for recursive model evaluation are used as assessment criteria. In [66], a genetic-algorithm-based method for generating Takagi-Sugeno models is proposed and tested on the SISO problem. The algorithm determines the number of rules, input partitioning, effective inputs of each rule and the conclusion function parameters. J_{MSE} is assessed for both training and validation data. It is not specified whether one-step-ahead or recursive evaluations are considered.

3.2. Data repositories for system identification and regression

The SISTA group of the Catholic University of Leuven collected data sets for system identification problems and provides them on the Internet [15]. The data majorly origin from process and mechatronic systems. At the time of writing, the 24 data sets reported in Table 1 were available in *DalSy*. The data sets are augmented by basic information such as a brief description of the process, the input/output quantities, and the sampling time. Furthermore, a reference is cited for each individual data sets. The data can be used to test, demonstrate and compare system identification methods. No general assessment criteria are specified. The use is e.g. reported in [55,38].

The IFAC Technical Committee 1.1. “Modelling, Identification and Signal Processing” provides five benchmark data sets on the committee’s web site [35]. One data set has been collected from an electronic circuit. The four other are artificial 30th order single-input single-output data sets with fast or slow dynamics and high or low signal to noise ratio.

Since 1997, the *Information Technology Laboratory* of the National Institute of Standards and Technology (NIST) offers statistical reference data sets as an easily accessible repository of reference data sets with certified values for a variety of statistical methods. The motivation for providing these is to permit assessing the accuracy of software for univariate statistics, analysis of variance, linear regression, and nonlinear regression [63]. The reference data sets include 27 sets for single-input single-output-type nonlinear regression problems [62]. These are augmented by a problem description, a proposed model, a description of the regression procedure and certified statistical results as well as a reference. The original problem was to exactly reproduce numerical results by applying a well-defined regression algorithm for the given data. Here, it is proposed to use the data as nonlinear regression benchmarks. Originally, the assessment criterion is whether the certified parameter values are exactly matched/reproduced.³

In the *Matlab Neural Network Toolbox* [7] and the corresponding demos, several benchmark data sets for function approximation are provided: The “Engine” data set with two inputs (engine speed, fueling level) and two outputs (torque, emission level), “Cholesterol” with 21 inputs (measured spectral components) and three outputs (cholesterol levels ldl, hdl, and vldl), “ball” as a dual sensor calibration problem with two inputs and one output, and “house” with 13 demographic attributes as inputs and the median price of a home in a neighborhood as single output. In addition, the “magnet levitation” data set is provided for system identification, where the magnet position is to be predicted from the control current.

In the *Matlab Fuzzy Logic Toolbox* [56] and the corresponding demos, the “gas mileage prediction” data set is a nonlinear regression problem from the UCI Machine Learning Repository. It has six inputs (number of cylinders, displacement, horsepower, weight, acceleration, year) and one output (miles per gallon). A data set generated from the Mackey-Glass time-delay differential equation is provided as a time-series prediction problem. The provided “dryer” data set is a single-input single-output system identification problem: from the voltage supply of a dryer, the dryer outlet temperature has to be predicted.

The 30 data sets recorded in Table 2 are included in the *Matlab Statistics Toolbox* [57].

The *UC Irvine Machine Learning Repository* [91] is well-known for its classification benchmark data sets. However, it also contains 27 data sets on regression problems.

The *DELVE repository* [16] of the Faculty for Computer Science of the University of Toronto, Canada, provides for 10 regression problem data sets. Of these, five are recommended for assessing and three for developing machine learning methods. Two are included as being established in literature. Two of the data sets in the first two groups are also included in the UCI machine learning repository.

³ i.e. with a precision of at least 4 to 5 digits.

Table 2
Data sets available in the *Matlab Statistics Toolbox*.

Chemical reaction data with correlated predictors	Cardiac arrhythmia data from the UCI machine learning repository
Measurements of cars, 1970–1982	Subset of <i>carbig.mat</i> , Measurements of cars, 1970, 1976, 1982
Breakfast cereal ingredients	Quality of life ratings for U.S. metropolitan areas
A version of <i>cities.mat</i> used for discriminant analysis	Exam grades on a scale of 0–100
Fisher's 1936 Iris data	Google Flu Trends estimated ILI (influenza-like illness) percentage for various regions of the US, and CDC weighted ILI percentage based on sentinel provider reports
Gasoline prices around the state of Massachusetts in 1993	Heat of cement vs. mix of ingredients
Bacteria counts in different shipments of milk	Simulated hospital data
1985 Auto Imports Database from the UCI repository	Ionosphere data-set from the UCI machine learning repository
Four-dimensional clustered data	Grade point average and LSAT scores from 15 law schools
Mileage data for three car models from two factories	Biochemical oxygen demand on five predictors
Recognition of Morse code distinctions by non-coders	Grouped observations on 4000 predictors
Dimensional run-out on 36 circular parts	Sample data for polynomial fitting
Popcorn yield by popper type and brand	Reaction kinetics for Hougen-Watson model
Scholastic Aptitude Test averages by gender and test (table)	Scholastic Aptitude Test averages by gender and test (csv)
NIR spectra and octane numbers of 60 gasoline samples	Simulated stock returns

The *WEKA* repository [98] contains 37 regression problems.

3.3. Cart with inverted pendulum

Motivation: The inverted pendulum benchmark, in particular the cart version, was used for teaching and research in control theory to stabilize open-loop unstable SISO systems. The first solution to this problem was described by [74] and then by [77]. This benchmark was considered in many references to solve the linear-quadratic optimal control problem around the unstable operating point [50] or as a nonlinear control problem in the full/an extended operating range.

Process description: The cart with inverted pendulum consists of a moveable carriage with one degree of freedom on which a pendulum is mounted and freely rotatable in driving direction (Fig. 2).

The carriage is driven by a motor that exerts a force F through belt drive transmission. The principal control objective is to swing up the pendulum from the stable equilibrium point to the unstable equilibrium point, and then balance the pendulum at the upright position, and further move the cart to a specified position on the track. The process can be described by two coupled nonlinear differential equations

$$\begin{aligned}\ddot{\Theta} &= \frac{1}{2l - mla \cos^2(\Theta)} (g \sin(\Theta) - mla \dot{\Theta}^2 \cos(\Theta) \sin(\Theta) - a \cos(\Theta)(u - f_c(\dot{x})) - \frac{d_{Mf}}{ml} \dot{\Theta}) \\ \ddot{x} &= \frac{2a}{2 - mla \cos^2(\Theta)} (ml \dot{\Theta}^2 \sin(\Theta) - \frac{1}{2} mg \cos(\Theta) \sin(\Theta) + u - f_c(\dot{x}) + \frac{1}{2l} \cos(\Theta) d_{Mf} \dot{\Theta})\end{aligned}\quad (32)$$

where $a = 1/(m+M)$, $f_c = F_c \operatorname{sgn}(\dot{x})$ is the Coulomb friction between the cart and the track and g denotes the gravity constant. The external force F is the input $u := F$ and is limited to $|F| \leq F_{\max}$. The angular position of pendulum θ is the output of this system.

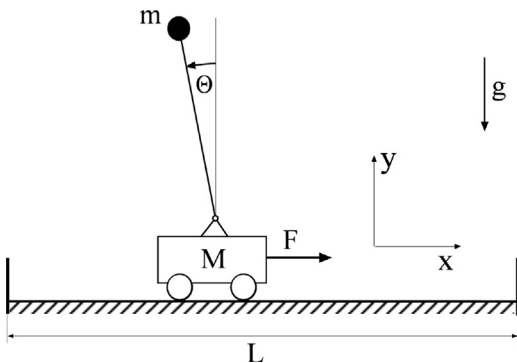


Fig. 2. Cart with inverted pendulum.

The parameters and variables of the cart inverted pendulum are recorded in Table 3.

Problem description: The control objective is to swing up the pendulum from the stable to the unstable equilibrium point, and then to stabilize the pendulum at the upright position, and further to move the cart to a desired position on the track. The general control problem is to guide the pendulum from any arbitrary initial condition to the upright equilibrium. The friction force $f_c(\dot{x})$ acts as an input disturbance.

Assessment criteria: An evaluation criterion is the required time to get the pendulum to the upright position. Furthermore, the disturbance compensation is evaluated. For friction disturbance tests, a tolerance band of $\varepsilon_{\Theta} = 0.1 \text{ rad}$ is specified. For assessing the controller robustness, the plant parameters m , M and l are changed up to $\pm 100\%$ and F_c by $\pm 20\%$.

Examples of reported use: In [5], a neural controller is trained using a single hidden-layer network as full-state feedback. A Takagi-Sugeno approach is applied in [95] to model and control the pendulum's angle by a four-rule TS system to design a PDC-control law without addressing the cart's position. The robustness of the closed-loop performance has been demonstrated with a 100% change of M , m and l to the nominal values. Here, the controller

performance is just verified by visual inspection of simulation results. In [100], a fuzzy controller based on single input rule modules (SIRMs) dynamically connected to a fuzzy inference model is presented. Simulation results show that the fuzzy controller can swing up the pendulum from the pending position and then stabilize the whole system in about three seconds.

3.4. Electro-mechanical throttle

Motivation: Electro-mechanical throttles are standard components in Diesel and Otto combustion engines and therefore million-fold deployed. To obtain robust low-cost components, construction is kept simple. This results in significant friction and other nonlinear effects.

Process description: Fig. 3 shows a technology scheme of a throttle. This mechatronic system consists of DC motor, gear box, return spring and throttle plate integrated in metal housing. A potentiometer is used to measure the plate's rotational position $\varphi(k)$ that can take values between 10° (closed) and 90° (open),

Table 3
Variables and parameters of cart with inverted pendulum.

Symbol	Description	Value	Unit
Θ	Angular position of the pendulum	–	rad
x	Linear displacement of the cart	–	m
u	Input: external force on the cart	–	N
m	Point mass of the pendulum	0.356	kg
M	Mass of the cart	4.8	kg
l	Distance from the joint to the mass point m	0.56	m
d_{Mf}	Viscous friction of the joint	0.035	Nms/rad
F_c	Coulomb friction coefficient	4.9	N
g	Gravitational constant	9.81	m/s ²
L	Total length of rail	2	m
F_{\max}	Maximum input value (actuator saturation)	120	N

which is considered as the output $y(k)$. The motor supply is a pulse width modulated signal. Its duty cycle (in %) is the system input $u(k)$.

In theory, a physical model can easily be derived for this process. In practice however, the friction can e.g. be state-dependent, the spring may have nonlinear characteristics, and some parts may be made of plastics such that deformations may occur. In addition, physical properties such as inertias or spring characteristics are typically not known.

Problem description: Original measurement data recorded with $T_0 = 10$ ms from a standard automotive throttle are publically available from [29] consisting of a multi-sine data set ($N = 10^4$) for identification and a “quasi” amplitude modulated pseudo random data set ($N = 2500$) for validation. Using this data, a parsimonious dynamical process model for simulation purposes is to be identified. Details of the electro-mechanical throttle, the test stand used to measure the data and a semi-physical model are provided in [69].

Assessment criteria: The prediction quality is assessed by J_{MAE} , J_{RMSE} , J_{BFR} and the frequency distribution of the residuals. The model complexity is assessed by the number of model parameters and qualitatively by the “sophistication” of the model structure.

Examples of reported use: In [70] a piece-wise affine (PWA) model is presented. k -means in the input signal space is used for grouping and assigning data to local models. Support vector machines are deployed to compute polyhedral boundaries of the local models. Initial local models are identified using the least squares method. These are optimized for parallel/recursive evaluation and provide a NOE model. A PWA model of NARX type is identified in [94] using least squares for parameter estimation and clustering in the parameter space instead of the signal space. In [3], a multi-layer perceptron network is used as model approach. In [71], a PWA model is compared with a semi-physical model that has been identified using a set of tailored test signals that differ from the benchmark data.

3.5. Servo-pneumatic actuator

Motivation: Servo-pneumatic actuators are used in a wide range of applications in industrial automation and manufacturing

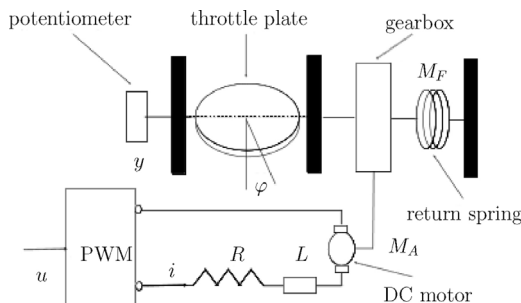


Fig. 3. Electro-mechanical throttle.

process control, because these are simply constructed, low cost and durable. However, the dynamics of pneumatic actuators is highly nonlinear. A number of characteristics, such as friction and the variation of actuator dynamics (as a result of large changes in load and piston position along the cylinder stroke) complicate the design of closed-loop controllers.

Process description: The system under consideration is a loaded two-way servo-pneumatic actuator (Fig. 4).

This consists of a piston, two variable volume chambers connected to a four-way servovalve, a pressure accumulator, and a pressure supply. The time-variant load mass $m_L(t)$ is rigidly mounted to the piston and moved only in the vertical direction x_k . The servovalve adjusts four orifice areas, which connect the supply pressure p_s , exhaust pressure p_e , and the chamber pressures p_I , p_{II} in order to produce the pressure difference between the chambers I and II that moves the load. The four orifice areas are adjusted by the servovalve supply voltage u_v . This process can be described by three coupled nonlinear differential equations

$$\begin{aligned} (m_L + m_k) \ddot{x}_k &= A_k (p_I - p_{II}) - F_f(\dot{x}_k), \\ \dot{p}_I [V_0 + A_k x_k] &= \kappa [R_g T_I (\dot{m}_2 - \dot{m}_1 - \dot{m}_{bp}) - A_k p_I \dot{x}_k], \\ \dot{p}_{II} [V_0 - A_k x_k] &= \kappa [-R_g T_{II} (\dot{m}_4 - \dot{m}_3 - \dot{m}_{bp}) + A_k p_{II} \dot{x}_k]. \end{aligned} \quad (33)$$

with

$$F_f(\dot{x}_k) = d_f \dot{x}_k + F_c \operatorname{sgn}(\dot{x}_k) \quad (34)$$

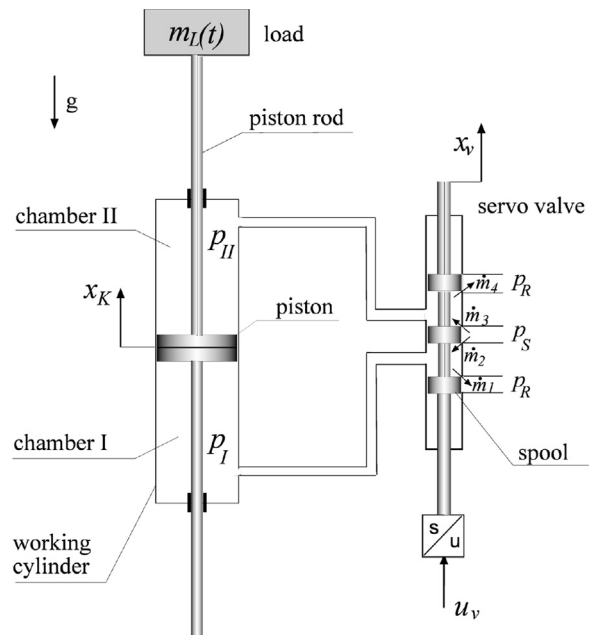


Fig. 4. Servo-pneumatic actuator with time-variant vertical load mass.

Table 4
Variables and parameters of pneumatic actuator model [81].

Symbol	Description	Value	Unit
\dot{m}_1, \dot{m}_2	Valve-controlled mass flow from/to chamber I	–	kg/s
\dot{m}_3, \dot{m}_4	Valve-controlled mass flow from/to chamber II	–	kg/s
\dot{m}_{bp}	Bypass mass flow between chamber I and II	–	kg/s
$p_{I,II}$	Pressure in chamber I, II	–	N/m ²
u_v	Servo valve control-signal voltage	–	V
\dot{x}_k	Actuator piston velocity	–	m/s
x_k	Actuator piston position	$ x_k \leq 0.125$	m
x_v	Servo valve displacement	–	m
A_k	Piston area	2.8×10^{-3}	m ²
d_{F_f}	Viscous friction coefficient	135	Ns/m
F_c	Coulomb friction coefficient	21	N
k_v	Servo valve gain	1×10^{-4}	m/V
m_k	Piston and rod mass	2.9	kg
m_L	Load mass	$\in [3, 9]$	kg
p_e	Exhaust pressure	1×10^5	Pa
p_s	Supply pressure	9×10^5	Pa
R_g	Ideal gas constant of air	8.314	Nm/(kg K)
$T_{I,II}$	Temperature of chamber I, II	293.15	K
u_v	Servo valve input	$-10, \dots, 10$	V
V_0	Half swept chamber volume	5×10^{-4}	m ³

as a static friction model. The dynamic transition between slip and stick has been neglected due to the strong time-varying behavior. The parameters and variables of the considered actuator are recorded in Table 4.

Problem description: The control variable is the piston position. Independent of the actual load, different set points have to be reached from different starting points. Additionally, a second control objective is the continuous reference tracking.

Assessment criteria: The quality of the position control is evaluated by the tracking behavior for a multi-step reference signal, ramp-shaped reference and sinusoidal reference signal. The performance criteria is the mean squared error (18), root mean squared error (19) and normalized mean squared tracking error (20). The load disturbance is generated by step-type and harmonic load mass variation of 200%. The disturbance rejection performance is measured for different operating points with (28) or (29).

Examples of reported use: It must be emphasized that in the following research papers only the same structure (double-acting cylinder, proportional servo valve, etc.) of the drive are used. The test-bed systems vary in size form and power consumption.

In [84], a self-tuning neural fuzzy controller is developed and implemented to control the piston position under vertical load. The control objective is to minimize J_{IAE} (13) and J_{PO} (14). In [53], an internal model controller (IMC) is combined with neural networks (NN). The NN is used as a supervisor to get the suitable control parameters. To assess the controller performance $J_{MSE_{Ref}}$ (18) is exploited. A Takagi-Sugeno approach is applied in [81] to control the piston position under variable pay loads. The overall control law is formulated as a PDC law wherein the robustness to frictional forces obtained with an additional integrator gain. The simple friction model used in (33) limits the achievable approximation quality, which motivates to alternatively identify nonlinear black box models. In [8], two different approaches of nonlinear black-box modeling (fuzzy systems and neural networks) are compared using case studies including the pneumatic actuator.

As in the previously described benchmarks, the pneumatic actuator received also attention in the conventional control community, for instance [12], [72], and [89].

3.6. Hydrostatic transmission in mobile working machines

Motivation: Hydrostatic transmissions have been widely used in mobile working machines and off-road vehicles such as wheel loaders, graders or tractors. The hydrostatic transmissions are gears

with high power density that offer important advantages like continuously variable transmission, maximum tractive force at low speeds and reversing without changing gear. As opposed to stationary industrial machines with fixed operational procedures, mobile working machines are subjected to a wide range of demands. Due to the highly diverse applications, extremely different environmental conditions are encountered. Nonetheless, reliability and operability must be guaranteed for all variations in environmental conditions. Based on the set of characteristic properties described in [28], it is evident that the problem of automatic control for mobile working machines falls under the class of really complex technical systems.

Process description: Fig. 5 shows the main hydraulic circuit of a hydrostatic transmission in a mobile working machine.

It consists of variable displacement hydraulic machines (pump and motor), speed and pressure sensors and an electronic control unit (ECU). The combustion engine is connected to a variable displacement pump, which is operated in a closed oil circuit with a variable displacement motor. The motor is connected to a fixed mechanical gear box, which drives the axle of the vehicle. The pressure levels (p_A, p_B) between the pump and the motor vary in both hoses (Fig. 5), depending on the operational situation (acceleration, near-constant speed, deceleration, etc.) and the parameters of the vehicle. Two electro-hydraulic control elements, enable to change the displacement of pump and motor. The displacement of the pump can be increased, decreased to zero or reversed, thus providing a range of forward, neutral and reverse vehicle speeds through the reversing of the flow direction in the closed circuit. The hydrostatic transmission can be described by four ordinary differential equations:

$$\begin{aligned}
 \dot{x}_1 &= -\frac{1}{\tau_{up}} x_1 + \frac{k_p}{\tau_{up}} u_1 \\
 \dot{x}_2 &= -\frac{1}{\tau_{um}} x_2 + \frac{k_M}{\tau_{um}} u_2 \\
 \dot{x}_3 &= \frac{10}{C_H} \left(\tilde{V}_{\max} x_1 \omega_p - \tilde{V}_{\max} x_2 x_4 - k_{leak} x_3 \right) \\
 \dot{x}_4 &= \frac{i_g^2 i_a^2 \eta_g \eta_{mh} \tilde{V}_{\max} p 10^{-4} x_2 x_3 - \tilde{d}_{vc} i_a^2 x_4 - T_{Lw} i_g i_a}{J_v}
 \end{aligned} \tag{35}$$

with the state vector

$$\mathbf{x} = [x_1, x_2, x_3, x_4]^T := [\tilde{\alpha}_p, \tilde{\alpha}_M, \Delta p, \omega_M]^T$$

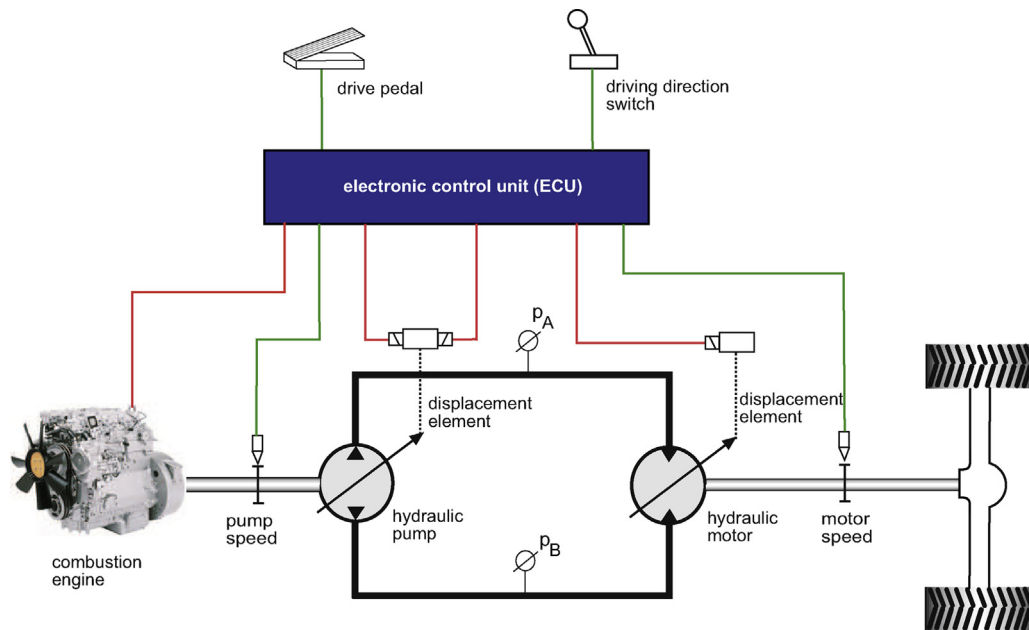


Fig. 5. Scheme of hydrostatic transmission in mobile working machines.

and the input vector

$$\mathbf{u} = [u_1, u_2]^T := [u_P, u_M]^T.$$

The variables and parameters are explained in Table 5.

Problem description: The control objective is the decoupled speed and torque control. In any driving situation (independent of the slope and road conditions), a given control performance must be achieved. For this, different reference signals such as ramps, sinusoidal curves and trapezoidal profiles are specified.

Assessment criteria: Control performance is measured by the steady state accuracy J_{IAE} (13) and root mean squared tracking error $J_{RMSE_{Ref}}$ (19) during acceleration/deceleration wherein the driving situation permanently changes. The controllers are compared by a driving profile containing relevant off- and on-road scenarios presented in Fig. 6. Further, the control effort is assessed by J_{peak_u} (22) and the integral squared control action (23).

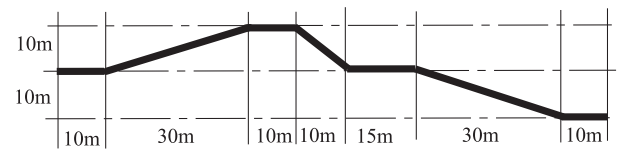


Fig. 6. Profile of a driving path.

Examples of reported use: In [79], a control-oriented model based on the class of Takagi-Sugeno fuzzy systems is presented. Using this model, a method for output feedback control design, taking into account the output matrix of the system model and the affine properties of the TS model structure, is presented in [46]. Based on the same model, a nonlinear observer design for pressure estimation in hydrostatic transmissions is investigated in [80]. In [19], an adaptive fuzzy sliding mode controller was developed for

Table 5
Variables and parameters of hydrostatic transmission model [79].

Symbol	Description	Value	Unit
x_1	Hydropump angle	$\in [-1, 1]$	–
x_2	Hydromotor angle	$\in [0, 1]$	–
x_3	Pressure difference	–	N/m ²
x_4	Hydromotor speed	–	rad/s
u_1	Control signal hydropump	$\in [-1, 1]$	–
u_2	Control Signal hydromotor	$\in [0, 1]$	–
T_{lw}	External load torque on wheel	–	Nm
ω_P	Hydropump speed	–	rad/s
C_H	Hydraulic capacitance	1840.8	mm ⁵ /N
\tilde{d}_{vc}	Viscous damping coefficient	0.33	Nms
i_a	Axle ratio	–23.3	–
i_g	Transmission ratio	–6.12	–
J_v	Moment of inertia of vehicle	16512	Nms ²
k_{leak}	Leakage coefficient	0.14	mm ³ /s bar
k_M	Static gain of motor displacement	283.33	–
k_P	Static gain of pump displacement	241.67	–
\tilde{V}_{max}^P	Max. displacement volume hydrop.	145	cm ³
\tilde{V}_{max}^M	Max. displacement volume hydrom.	170	cm ³
η_g	Gearbox efficiency	0.98	–
η_{mh}	Hydro-mechanical efficiency	0.697	–
τ_{uP}	Time constant hydropump	0.13	s
τ_{uM}	Time constant hydromotor	0.22	s

Table 6
Variables and parameters of three-tank system [41].

Symbol	Description	Value	Unit
x_1	Water level of tank 1	$\in [0, h_{\max}]$	m
x_2	Water level of tank 2	$\in [0, h_{\max}]$	m
x_3	Water level of tank 3	$\in [0, h_{\max}]$	m
u_1	Incoming flow rate tank 1	$\in [0, q_{1\max}]$	m ³ /s
u_2	Incoming flow rate tank 2	$\in [0, q_{2\max}]$	m ³ /s
A_T	Cross-section of tank T_i , $i = 1, 2, 3$	$154 \cdot 10^{-4}$	m ³
A_O	Cross-section area of valve V_i , $i = 1, 2, 3$	$0.5 \cdot 10^{-4}$	m ³
A_C	Cross-section area of valve V_{12}, V_{23}	$0.5 \cdot 10^{-4}$	m ³
h_{\max}	Max. Water level of tank T_i , $i = 1, 2, 3$	0.62	m
$q_{i\max}$	Max. Flow rate of pump $i = 1, 2$	$100 \cdot 10^{-6}$	m ³ /s
α_O	Flow coefficient of valve V_{O_i} , $i = 1, 2, 3$	0.56	–
α_C	Flow coefficient of valve V_{C_i} , $i = 1, 2$	0.48	–
g	Gravitational constant	9.81	m/s ²

speed control of mobile working machines to cope with nonlinearities in the displacement unit of the pump/motor and load changes caused by rough roadway surface and variation of the slope. Until now the control performance is verified by visual inspection of simulation [19], [46], [79] and experimental results [80]. The presented benchmark received also attention in the conventional control community, for instance in [48], [65], and [6].

3.7. Three-tank-system

Motivation: The three-tank-system (Fig. 7) can be viewed as a prototype of many industrial process control applications, e.g. in chemical and petrochemical plants or oil and gas systems. The typical control problem is to track level in the first and second tank by the two input flows q_1 and q_2 . Moreover, the three-tank process is often used as a benchmark for fault diagnosis and isolation as well as fault tolerant control.

Process description: The benchmark system consists of three cylindrical tanks T_1 , T_2 , and T_3 , each of cross sectional area A_T , see Fig. 7.

These tanks are connected to each other through pipes of cross sectional area A_C . Both connecting pipes can be closed by valve V_{C1} and V_{C2} . The system includes a total of four outlet valves: one in each tank T_1 , T_3 and two in T_2 . Each outlet valve V_{O_i} has a cross-section of A_O in the open state, in which the outlet flow goes to the reservoir and may be pumped into T_1 and T_2 by pump P_1 and P_2 with mass flow-rate $q_1(t)$ and $q_2(t)$, respectively. The water level in each tank T_i , $i = 1, \dots, 3$ is represented by $h_i(t)$. The maximum water level in each tank can be denoted by h_{\max} . The incoming mass flows $q_1(t)$, $q_2(t)$ are considered as process inputs and the water levels

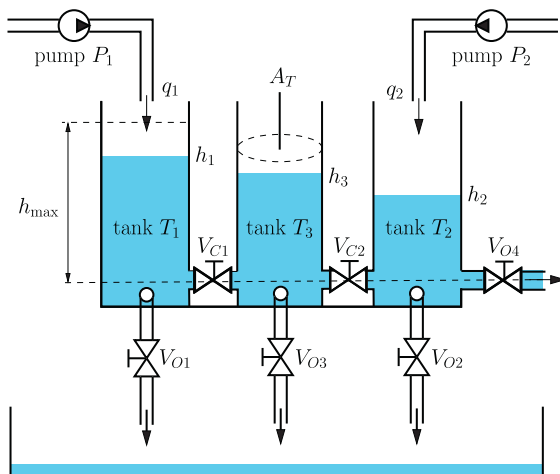


Fig. 7. Three-tank-system.

$h_1(t)$, $h_2(t)$, $h_3(t)$ define the process state. With $x_i := h_i$, $i = 1, \dots, 3$, $u_1 := q_1$, and $u_2 := q_2$ the nonlinear model of the three-tank-system becomes

$$\begin{aligned}\dot{x}_1 &= \frac{1}{A_T} (-A_C \alpha_C \operatorname{sgn}(x_1 - x_3) \sqrt{2g|x_1 - x_3|} + u_1) \\ \dot{x}_2 &= \frac{1}{A_T} (+A_C \alpha_C \operatorname{sgn}(x_3 - x_2) \sqrt{2g|x_3 - x_2|} + u_2) \\ \dot{x}_3 &= \frac{1}{A_T} (+A_C \alpha_C \operatorname{sgn}(x_1 - x_3) \sqrt{2g|x_1 - x_3|} \\ &\quad - A_C \alpha_C \operatorname{sgn}(x_3 - x_2) \sqrt{2g|x_3 - x_2|})\end{aligned}\quad (36)$$

with flow coefficients $0 < \alpha_O, \alpha_C < 1$. Note that in the nominal case, it is assumed that the valves V_{O1} , V_{O2} and V_{O3} are closed. Table 6 records variables and parameters.

Assessment criteria: The main objective is to control the level of water in each tank under various disturbances. However, in literature, different scenarios have been examined. A frequently studied case is the output tracking control of $y_1 := x_1$ and $y_2 := x_2$ with a multi-step reference signal $\mathbf{r} = [r_1, r_2]^T$. For the performance measurement the RMSE criteria (19) or the Integrated-Absolute-Error (13) is used.

Examples of reported use: In [10], a control design via the combination of a neural predictive controller and the neuro-fuzzy controller type of ANFIS is presented. The performance of each controller are compared by the IAE criteria. In [11], a fuzzy adaptive control algorithm is presented. It belongs to the class of direct model reference adaptive techniques based on a Takagi Sugeno fuzzy model of the plant. A support-vector-machine-based generalized predictive control (GPC) scheme is applied to the three-tank-system in [36]. Experimental results have shown that the proposed method can handle the control task successfully for different reference trajectories. Further, an European project COSY (Control of Complex Systems) has considered the three-tank system as a benchmark for all partners [32]. It is not specified which performance measurement is to be used.

In particular, the three-tank process is often introduced as a benchmark for fault diagnosis and isolation (FDI) and fault tolerant control (FTC). In [67], a sensor FDI scheme has been constructed using a self-organizing map (SOM) as feature cluster module and active FTC has been achieved by switch mode control using Mamdani fuzzy logic controller. In [2], a Takagi-Sugeno fuzzy observer is used to estimate the tank levels by elimination of unknown inputs. An application of FTC using weighted fuzzy predictive control is proposed in [58].

3.8. Continuously operated bio-chemical reactor

Introduction: Continuously operated bio-reactors are frequently used in bio-chemical plants. In this section, the bio-reactor

from [93,4] will be introduced. A simplified model was used in order to obtain a simple, yet challenging, control problem.

Process description: The cell growth in the reactor only depends on the fed nutrient. The target quantity is the cell mass yield. The process can be described by two coupled nonlinear differential equations:

$$\begin{aligned}\dot{C}_1(t) &= -C_1(t) u(t) + C_1(t) (1 - C_2(t)) e^{C_2(t)/\Gamma} \\ \dot{C}_2(t) &= -C_2(t) u(t) + C_1(t) (1 - C_2(t)) e^{C_2(t)/\Gamma} \\ \frac{1 + \beta}{1 + \beta - C_2(t)}\end{aligned}\quad (37)$$

C_1 and C_2 are dimensionless cell mass and substrate (nutrient) conversion, respectively. C_2 is defined as $C_2 = (S_F - S)/S_F$ with the substrate concentration S_F in the feed and the substrate concentration S in the reactor. They are bounded between zero and unity. The quantity u is the feed flow rate, which equals the outflow from the tank. The parameters Γ and β determine the rate of cell formation and nutrition consumption, respectively. The nominal values are $\Gamma = 0.4$ and $\beta = 0.02$, which provide for a Hopf bifurcation at $u = 0.829$. Dependent on the operating point, the reactor exhibits stable behavior, instable behavior or limit-cycles. Moreover, two different values of the input feed rate u can lead to the same cell mass yield (C_1). Control is applied each 0.5 dimensionless time units.

Also a discrete-time representation is introduced: The system equations are integrated with a forward Euler scheme with step size of $\Delta = 0.01$ dimensionless time units. Using an equidistant sampling time of $50 \cdot 0.01$ time units, which corresponds to the update time of sensor and control signal, provides for⁴

$$\begin{aligned}C_1(k+1) &= C_1(k) + \Delta [C_1(k) ((1 - C_2(k)) e^{C_2(k)/\Gamma} - u(k))] \\ C_2(k+1) &= C_2(k) + \Delta \left[C_1(k) (1 - C_2(k)) e^{C_2(k)/\Gamma} \right. \\ &\quad \left. \frac{1 + \beta}{1 + \beta - C_2(k)} - C_2(k) u(k) \right]\end{aligned}\quad (38)$$

Problem description: The bio-reactor model can be used to test nonlinear system identification and nonlinear control algorithms. Proposed problems are (i) control about the point $u = 0.75$, which is open-loop stable, (ii) control about the point $u = 1.25$, which is open-loop unstable, and (iii) control of the set-point change from $u = 0.769$ corresponding to $C_1 = 0.1236837$ to a target value increased by 0.05. The later means changing operation from a stable region to the domain of attraction of the limit cycle [92].

Assessment criteria: For assessing control, the tracking behavior for a multi-step signal is proposed. For assessing the controller robustness, the plant parameters are changed to $\Gamma = 0.456$ and $\beta = 0.016$. Performance should be assessed for the noise-free case and for Gaussian measurement noise with standard deviation of $\sigma = 0.01$ that is added to both state components [24,68]. The performance criterion is the squared control deviation ($N \cdot J_{\text{MSEdist}}$).

Examples of reported use: In [24,68] MLP-based process models and a neural controller are trained. The model's one-step-ahead predictive is visually inspected. The bio-reactor model in discrete-time representation is utilized in [13] to train fuzzy models. In [30], the continuous-time representation is used to demonstrate an adaptive control algorithm that uses an affine radial basis function network for modeling the plant dynamics. So do [21] to

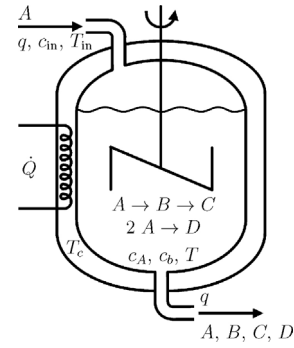


Fig. 8. Continuously-operated stirred tank reactor (CSTR) with cooling jacket [93].

test a neural-network-based control method. The previous references just visually assess the time series of measurements vs. model predictions and reference vs. controlled variable/control error. [14] utilize the continuous-time representation to train neural networks. The percentage of five-step-ahead prediction within the calculated prediction intervals is assessed for the test-data set. [37] use this for a support-vector-machine-based control scheme, which is a further development of ANFIS.

3.9. Continuously stirred chemical reactor

Introduction: Continuously operated stirred tank reactors (CSTR) are processing units that are frequently used in chemical plants. If e.g. parallel and consecutive reactions occur, the resulting process dynamics are difficult to control. This has made CSTR a popular benchmark problem for nonlinear modeling and control. Several reactor models have been published of which the Klatt-Engell reactor will be presented, see Fig. 8.

Process description: The Klatt-Engell reactor problem was originally published in [42,44,43]. In [93], the problem description was augmented with details for a control benchmark, the latter description is the major reference for the following description. The CSTR has a cooling jacket. The main reaction $A \rightarrow B$ converts reactant A to the desired product B . It is accompanied by a side reaction $2A \rightarrow D$ and a follow-up reaction $B \rightarrow C$ that both produce undesirable byproducts (C, D). The material and energy balances provide for:

$$\begin{aligned}\dot{c}_A &= -k_1(T) c_A - k_2(T) c_A^2 + (c_{in} - c_A) u_1, \\ \dot{c}_B &= k_1(T) (c_A - c_B) - c_B u_1, \\ \dot{T} &= h(c_A, c_B, T) + \alpha (T_c - T) + (T_{in} - T) u_1, \\ \dot{T}_c &= \beta (T - T_c) + \gamma u_2,\end{aligned}\quad (39)$$

with

$$\begin{aligned}h(c_A, c_B, T) &= -\delta (k_1(T) (c_A \Delta H_{AB} + c_B \Delta H_{BC}) \\ &\quad + k_2(T) c_A^2 \Delta H_{AD}).\end{aligned}\quad (40)$$

c_{in} is the concentration of reactant A in the feed, c_A and c_B are the concentration of A and B , respectively, in the reactor. T and T_c denote reactor and coolant temperature, respectively. u_1 and u_2 are reaction rate coefficients. α, β, γ , and δ are quantities composed each from several physical parameters, see [43] for details. The reaction kinetics depend on the temperature T :

$$k_i(T) = k_{i0} \exp \left(\frac{-E_i}{T + 273.15} \right), \quad (41)$$

⁴ The difference equations were taken from [24,68] due to errors in the original paper [93].

Table 7
Model parameter and set-point values for Klatt–Engell reactor.

$c_{A,SP1} = 3517.5 \text{ mol/m}^3$	$c_{A,SP2} = 2985 \text{ mol/m}^3$
$c_{B,SP1} = 740 \text{ mol/m}^3$	$c_{B,SP2} = 960 \text{ mol/m}^3$
$c_{in} = 5100 \pm 600 \text{ mol/m}^3$	$T_{in} = 104.9 \text{ K}$
$E_1 = 9758.3$	$E_2 = 8560$
$\Delta H_{AB} = 4.2 \text{ kJ/mol}$	$\Delta H_{BC} = -11.0 \text{ kJ/mol}$
$\Delta H_{AD} = -41.85 \text{ kJ/mol}$	
$k_{10} = 1.287 \cdot 10^{12} \text{ h}^{-1}$	$k_{20} = 9.043 \cdot 10^6 \text{ m}^3/\text{mol}$
$T_{SP1} = 87 \text{ K}$	$T_{SP2} = 106 \text{ K}$
$T_{c,SP1} = 79.8 \text{ K}$	$T_{c,SP2} = 100.7 \text{ K}$
$u_{1,SP1} = 8.256 \text{ h}^{-1}$	$u_{2,SP1} = -6.239 \text{ MJ/h}$
$u_{1,SP2} = 18.037 \text{ h}^{-1}$	$u_{2,SP2} = -4.556 \text{ MJ/h}$
$\alpha = 30.8285 \text{ h}^{-1}$	$\beta = 86.688 \text{ h}^{-1}$
$\gamma = 0.1 \text{ K/kJ}$	$\delta = 3.556 \cdot 10^{-4} \text{ m}^3 \text{ K/kJ}$

where the E_i are activation energy parameters. The (manipulated) inputs are the flow rate q scaled to the reactor volume V_R :

$$u_1 = \frac{q}{V_R} \quad \text{subject to the constraint} \quad 5 \leq u_1 \leq 35 \text{ h}^{-1} \quad (42)$$

and the cooling capacity

$$u_2 = \dot{Q} \quad \text{subject to the constraint} \quad -8.5 \leq u_2 \leq 0 \text{ MJ/h.} \quad (43)$$

The parameter values and the two considered set points are recorded in Table 7.

The system state is $\mathbf{x}^T = [c_A, c_B, T, T_c]$. The (controlled) outputs are: $y_1 = c_B$ and $y_2 = T$. (Only T and T_c are measured in the original problem [93], but neither c_A , c_B or disturbance c_{in} . Furthermore, the heat transfer coefficient γ is assumed to be unknown. Part of the problem is to estimate these four quantities.)

Problem description: The Klatt–Engell reactor is proposed as nonlinear control problem. The task is to perform a transition between set-point SP_1 and SP_2 as recorded in Table 7: at first for nominal conditions and secondly for a step-type disturbance of the input concentration c_{in} applied 1 min. after transition start, at t_0 :

$$c_{in}(t) = \begin{cases} 5100 \text{ mol/m}^3, & t - t_0 < 1 \text{ min}, \\ 4500 \text{ mol/m}^3, & t - t_0 \geq 1 \text{ min}. \end{cases} \quad (44)$$

Measurement noise is modeled as an uniformly distributed random number in $[-0.1 \text{ K}, 0.1 \text{ K}]$ that is added to both temperature signals.

Assessment criteria: The control performance is firstly assessed by the settling time ($\pm 0.5\%$ tolerance band), overshoot and steady state deviation. Secondly, the sum of squared scaled control deviation

$$\sum_{k=0}^N \bar{e}_j^2(k) \quad \text{with} \quad \bar{e}_j(k) = \frac{y_j(k) - y_{SP2,j}}{y_{SP2,j}}, \quad j = 1, 2 \quad (45)$$

similar to (21) and the sum of squared scaled control activity

$$\sum_{i=k}^N (\tilde{u}_j(k) - \tilde{u}_j(k-1))^2 \quad \text{with} \quad \tilde{u}_j(k) = u_j(k)/u_{SP2,j} \quad (46)$$

as normalized version of (23) are assessed for $N+1$ equally spaced time instances ($N=720$), starting from the beginning of the transition. The scaling is used to ease comparing different outputs and input, respectively.

Examples of reported use: The Klatt–Engell reactor is used e.g. in [49] in context of a method for model-based predictive control that bases on piecewise affine (PWA) models. The PWA state variable models are obtained by linearizing in several points and deriving local model boundaries from the corresponding Voronoi diagram. The model is assessed by the integral squared deviation of the right sides of the true system's and the model's state equations (norm not specified) for different test scenarios. In addition,

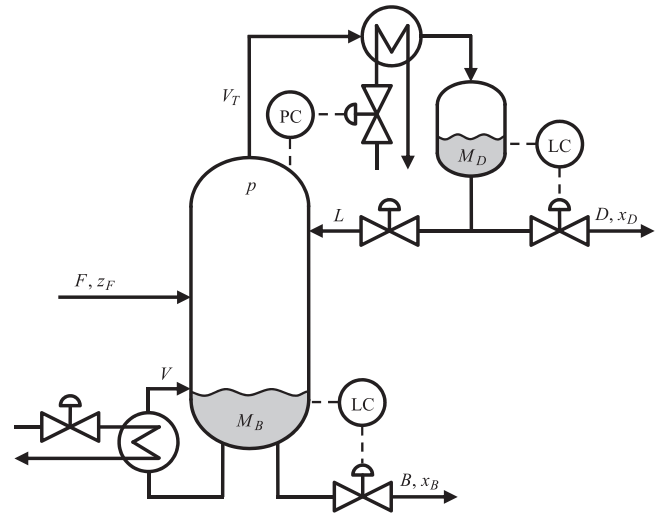


Fig. 9. Distillation column LV-configuration [87].

the state variables' trajectories for the true system and the model are visually analyzed. The control performance is assessed by a weighted superposition of a p -norm applied to the state variables' tracking error and the control action. The computational efforts to calculate the control action is also assessed. In [31], it is used as test example for a feedforward control design method that addresses in particular transitions between multiple stationary set-points.

3.10. Continuously operated binary distillation column

Introduction: Distillation columns are common units in chemical plants. They are multi-variable systems and show complex non-intuitive nonlinear behavior. Distillation columns are often used as application example for nonlinear system identification and control methods. Some physical models have become benchmark problems including the models reported in [97], [54] and [87]. A Matlab model "column A" is provided by Prof. Sigur Skogestad on the Internet [88]; that is why the latter has been selected for presentation in the following.

Process description: The distillation "column A" separates a binary mixture. It has $N_T = 41$ stages and includes a total condenser and a reboiler. Modeling assumptions are: constant pressure, negligible vapor holdup, total condenser, constant molar flows, equilibrium on all stages with constant relative volatility and linearized liquid flow dynamics. A version without control is provided with four manipulated inputs, three disturbances, four outputs and 82 states ("4 × 4column"): The four manipulated variables are recycle, boilup, distillate and bottoms product flow rate. The three disturbances are feed rate, feed composition and feed liquid fraction. The four outputs are top and bottom product composition as well as reboiler and condenser holdup. The first two outputs characterize the two product streams while the latter two have to be considered for operational feasibility [86]. In addition, models that include control loops are provided. E.g., a design in "LV-configuration" is available (Fig. 9), where recycle and boilup flow rate are used to control reboiler and condenser holdup. This reduces the system to two manipulable inputs and two outputs ("2 × 2column"). The model description originates from the website [88], where the simulation model is provided. The following set of equations applies to all stages of the column except top (condenser), feed and bottom (reboiler) stage. Variables and parameters are described in Table 8.

Table 8

Variables and parameters of “column A” model.

Quantity	Description	Unit
D/B	Distillate top/bottoms product flowrate	kmol/min
F/z_F	Feed rate / feed composition	kmol/min/mole fraction
i	Stage no. (1 = bottom, $N_F = 21$ = feed stage, $N_T = 41$ = total condenser)	–
L_i/V_i	Liquid/vapor flow from stage i	kmol/min
M_i	Liquid holdup on stage i	kmol
$L = L_T$	Reflux flow	kmol/min
q_F	Fraction of liquid in feed	–
τ_{aul}	Time constant for liquid flow dynamics on each stage	min
$V = V_B$	Boilup flow	kmol/min
x_i/y_i	Liquid/vapor composition of light component on stage i	mole fraction
α	Relative volatility between light and heavy component	–
λ	Constant for effect of vapor flow on liquid flow	–

The total material balance for stage i provides for:

$$\frac{dM_i}{dt} = L_{i+1} - L_i + V_{i+1} - V_i \quad (47)$$

and the material balance for the light component on each stage i for:

$$\frac{d(M_i x_i)}{dt} = L_{i+1} x_{i+1} + V_{i-1} y_{i-1} - L_i x_i - V_i y_i, \quad (48)$$

which yields the derivative of the liquid mole fraction:

$$\frac{dx_i}{dt} = \frac{(d(M_i x_i)/dt) - (x_i (dM_i/dt))}{M_i}. \quad (49)$$

Due to the vapor-liquid equilibrium on each stage the following holds:

$$y_i = \frac{\alpha x_i}{1 + (\alpha - 1) x_i}. \quad (50)$$

Assuming constant molar flow and neglecting vapor dynamics provides for the vapor flow $V_i = V_{i-1}$, except for the feed stage with $V_{N_F} = V_{N_F-1} + (1 - q_F) F$. The simplified relationship for the liquid flow is (the implemented model assumes $\lambda = 0$):

$$L_i = L_{0_i} + \frac{M_i - M_{0_i}}{\tau_{\text{aul}}} + (V - V_0)_{i-1} \lambda. \quad (51)$$

For the feed at stage $i = N_F = 21$ the following holds:

$$\begin{aligned} \frac{dM_i}{dt} &= L_{i+1} - L_i + V_{i-1} - V_i + F, \\ \frac{d(M_i x_i)}{dt} &= L_{i+1} x_{i+1} + V_{i-1} y_{i-1} - L_i x_i - V_i y_i + F z_F, \end{aligned} \quad (52)$$

for the total condenser at stage $i = N_T = 41$ ($M_{N_T} = M_D$, $L_{N_T} = L_T$):

$$\begin{aligned} \frac{dM_i}{dt} &= V_{i-1} - L_i - D, \\ \frac{d(M_i x_i)}{dt} &= V_{i-1} y_{i-1} - L_i x_i - D x_i, \end{aligned} \quad (53)$$

and for the reboiler at stage $i = 1$ ($M_1 = M_B$, $V_1 = V_B = V$)

$$\begin{aligned} \frac{dM_i}{dt} &= L_{i+1} - V_i - B, \\ \frac{d(M_i x_i)}{dt} &= L_{i+1} x_{i+1} - V_i y_i - B x_i. \end{aligned} \quad (54)$$

The nominal conditions are recorded in Table 9.

Problem description: The first principles distillation column model is used as benchmark problem for data-driven modeling as well as for control.

Assessment criteria: No specific criteria are specified.

Examples of reported use: In [11, example 4.2], a discrete-time fuzzy model is identified for the “2 × 2 column” from 10⁵ data sets

that were sampled with 120 s and divided into four data sets à 2000 observations for estimation and four data sets à 500 observations for validation. The model performance is assessed with J_{SSE} individually for both outputs for recursive model evaluation wrt. the full data sets with 10⁵ samples in total. In [59] 8000 data sets are used for the same approach. The model performance is assessed with J_{RMSE} and J_{VAF} on the validation data set. In [76], a fuzzy model for the “4 × 4 column” is identified from 600 data sets (equally divided into data for estimation and validation). J_{RMSE} on the training data set is used as assessment criterion. In [34] multi-model LPV models are identified for the “2 × 2 column” using 34 000 or 58 000 data sets that were sampled with 60 sec. The model performance is assessed with J_{VAF} determined for one-step-ahead and recursive model evaluation for the validation data set. In [75] the “2 × 2 column” is used to demonstrate online identification of neuro-fuzzy networks. J_{MSE} is used as assessment criterion.

3.11. ALSTOM Gasifier Control Benchmark II

Introduction: In the late 90s, the ALSTOM Power Technology Centre, Wheatstone/England, provided three linear process models for a coal gasifier that were derived from a nonlinear plant model for a control benchmark problem. In 2002, a nonlinear plant model was provided and the ALSTOM gasifier control benchmark problem II was announced.

Process description: The gasification process (Fig. 10) is part of a novel small-scale power generation plant based on the air-blown gasification cycle. An experimental facility exists that was used to provide data for model validation. The gasifier is a nonlinear multi-variable system with strong interactions and stiff dynamics: The five controllable inputs are the flow rates of char, air, coal,

Table 9

Nominal values for operating “column A”.

Value	Description	Unit
$B = 0.5$	Bottoms product flowrate	kmol/min
$D = 0.5$	Distillate product flowrate	kmol/min
$F = 1$	Feed rate	kmol/min
$L_T = 2.706$	Reflux flow	kmol/min
$M_{0i} = 0.5$	Liquid holdup for all stages	kmol
$q_F = 1$	Feed liquid fraction (i.e., saturated liquid)	–
$z_F = 0.5$	Feed composition	mole fraction
$\tau_{\text{aul}} = 0.063$	Time constant for the liquid flow dynamics on each stage (except reboiler and condenser)	min
$V = 3.206$	Boilup	kmol/min
$x_B = x_1 = 0.01$	Bottoms product composition	mole fraction
$y_D = x_{N_T} = 0.99$	Distillate product composition	mole fraction

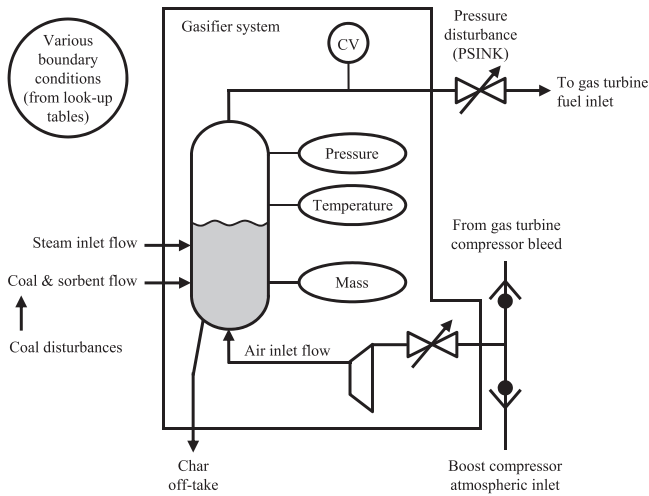


Fig. 10. Technology schematic of gasifier [18].

steam and limestone. The two disturbance inputs are sink pressure and coal quality. The four controlled outputs are fuel gas calorific value, bed-mass, fuel gas pressure and fuel gas temperature. As limestone is used to absorb sulfur in the coal, its flow rate must remain in fixed ratio to the coal flow. For this reason, there are only four independent controllable inputs. Two models are provided on the Internet by Dr. Roger Dixon encapsulated as Matlab C-code S-function [17]: An open-loop plant and a plant with a PI multi-variable controller. The later provides the baseline performance for comparisons.

Problem description: The control objective is disturbance rejection. The controllable inputs are subject to constraints on magnitude and rate of change. They are specified in detail in [18] and result from physical limitations of the actuators.

Assessment criteria: The performance of the closed-loop response to step-type and harmonic pressure changes as well as to load and coal quality changes is to be assessed. For all test scenarios, detailed test signals are specified. The objective is to maintain the controlled variables within given limits and as close as possible to their nominal values. For the pressure disturbance tests, tolerance bands are specified. For comparison, design of and results for a linear multi-variable PI-controller are presented that have been optimized for operation with 100% load. The models identified for controller design are assessed using R^2 defined in (6) on training and validation data sets. Control performance is assessed by the maximum and by the integral absolute deviation of the controlled variables from their respective reference value in different test cases.

Examples of reported use: In [96], a Wiener model consisting of a serial connection of a linear state-space model and a static single-hidden-layer feed-forward neural network is identified for the gasifier. It is used as prediction model in a nonlinear model-predictive controller. For this purpose, the four independent inputs of the simulation model are simultaneously excited with PRBS signals. The plant signals are sampled with 1 sec. and 2000 data sets are recorded for identification and 3000 for validation. In [83] a nonlinear Wiener model is identified for the one output variable showing strong nonlinear behavior and a linear state space model for the other three outputs. This model is used for model-predictive control of the gasifier. In [23], a genetic algorithm is used for optimal input-output pairing for PID-control loops as well as for determining PID controller and cross-coupling gains between the four control loops. The provided nonlinear simulation model is used for the required computations. In [85], a genetic algorithm is used to thin out a full

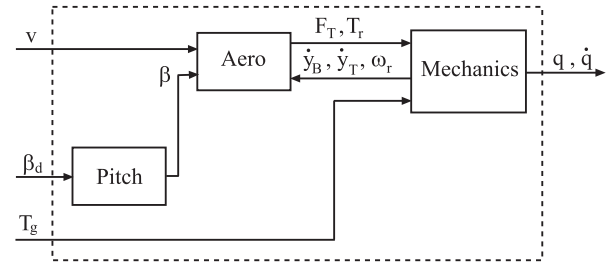


Fig. 11. Submodels of the complete wind turbine model with the respective inputs and outputs. v : wind speed; F_T, T_r : rotor thrust and torque; \dot{y}_B, \dot{y}_T : tower top and blade tip velocities; ω_r : rotor angular velocity; T_g : generator torque; β : pitch angle; β_d : demanded pitch angle.

cross-coupling network that was added to single-loop PI controllers from the benchmark package.

3.12. Wind turbine

Motivation: Modern wind turbines are complex systems with large flexible structures operating under turbulent, unpredictable, sometimes extreme weather conditions, they are connected to the electrical grid with changing frequency and voltages. Wind turbines have to adapt to the changing environments and thus the used control strategies have a significant impact on their reliability, availability, and efficiency.

Process description: To validate the control strategies, two different types of simulation models are increasingly used:

Control-oriented model: The control-oriented model is introduced in [9] and a Takagi-Sugeno formulation based on this is presented in [27]. The model consists of three submodels: The mechanical submodel, which includes drive-train and structure, the aerodynamics submodel, and the pitch actuator submodel. These submodels are coupled, which is illustrated in Fig. 11. All model parameters are described in Table 10.

For the *mechanical submodel*, four degrees of freedom are considered: rotor and generator rotation with a torsion-flexible shaft in between, as well as tower fore-aft and blade flapwise bending, which are modeled as translational motions of the tower top and the blade tip, respectively. The degrees of freedom of the mechanical submodel are illustrated in Fig. 12.

The vector of the generalized coordinates is therefore given by $\mathbf{q} = [y_T, y_B, \theta_r, \theta_g]^T$, where y_T and y_B denote the tower top and blade tip deflections, while θ_r and θ_g denote the rotor and generator rotational angles. The vector of external forces is given by $\mathbf{f} = [F_T, F_T, T_r, -T_g]^T$ where F_T denotes the aerodynamic rotor thrust force, T_r

Table 10
Parameters of wind turbine model.

Symbol	Description	Value	Unit
m_T	Effective mass of nacelle-tower motion	436865	kg
m_B	Effective mass of blade-tip motion	4435	kg
N	Number of blades	3	–
J_r	Rotor inertia	38759227	kg m ²
J_g	Generator inertia	5025347	kg m ²
d_T	Fore-aft tower damping constant	7×10^4	Ns/m
d_B	Flap-wise blade damping constant	2×10^4	Ns/m
d_s	Drivetrain damping constant	6215000	Nm s
k_T	Effective tower fore-aft stiffness parameter	1981900	N/m
k_B	Effective blade flap-wise stiffness parameter	40000	N/m
k_s	Drivetrain stiffness parameter	867637000	Nm
ρ	Air density	1.225	kg/m ³
R	Rotor radius	63	m
τ	Delay time constant for pitch dynamics	0.1	s

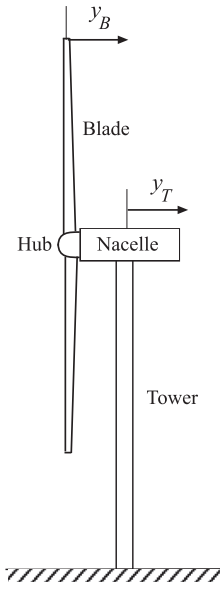


Fig. 12. Schematic side-view of a wind turbine.

the aerodynamic rotor torque and T_g the applied generator torque. The mechanical submodel can be written in matrix form as

$$\mathbf{M}\ddot{\mathbf{q}} + \mathbf{D}\dot{\mathbf{q}} + \mathbf{K}\mathbf{q} = \mathbf{f}, \quad (55)$$

where the mass matrix \mathbf{M} , the damping matrix \mathbf{D} and the stiffness matrix \mathbf{K} are given as

$$\begin{aligned} \mathbf{M} &= \begin{bmatrix} m_T + N & m_B & N & m_B & 0 & 0 \\ N & m_B & N & m_B & 0 & 0 \\ 0 & 0 & 0 & J_r & 0 & 0 \\ 0 & 0 & 0 & 0 & J_g & 0 \end{bmatrix}, \\ \mathbf{D} &= \begin{bmatrix} d_T & 0 & 0 & 0 & 0 & 0 \\ 0 & N & d_B & 0 & 0 & 0 \\ 0 & 0 & d_S & -d_S & 0 & 0 \\ 0 & 0 & -d_S & d_S & 0 & 0 \end{bmatrix}, \\ \mathbf{K} &= \begin{bmatrix} k_T & 0 & 0 & 0 & 0 & 0 \\ 0 & N & k_B & 0 & 0 & 0 \\ 0 & 0 & k_S & -k_S & 0 & 0 \\ 0 & 0 & -k_S & k_S & 0 & 0 \end{bmatrix}, \end{aligned} \quad (56)$$

with the tower and blade mass m_T and m_B , the rotor and generator inertia J_r and J_g , and the number of rotor blades N . k_T and k_B denote the effective stiffness coefficients for the tower top and blade tip velocity. d_T and d_B denote the damping coefficients for tower and blade. k_S and d_S denote the torsional stiffness and damping coefficients of the shaft. As gearbox dynamics are not considered here, a gearbox ratio can easily be included into the model by appropriately modifying the generator inertia J_g and the generator torque T_g .

The aerodynamics submodel comprises the expressions for the rotor thrust force F_T and the rotor torque T_r . These depend on the aero maps C_T and C_Q for the thrust and torque coefficient [25]:

$$\begin{aligned} F_T &= \frac{1}{2} \rho \pi R^2 C_T(\lambda, \beta) v_{\text{eff}}^2, \\ T_r &= \frac{1}{2} \rho \pi R^3 C_Q(\lambda, \beta) v_{\text{eff}}^2, \end{aligned} \quad (57)$$

where ρ denotes the air density, R the rotor radius, and β the collective pitch angle. $\lambda = \omega_r R / v_{\text{eff}}$ denotes the tip speed ratio. $v_{\text{eff}} = v - (\dot{y}_T + \dot{y}_B)$ is the effective wind speed at the rotor, where the wind speed v is modified by the absolute movement of the blade.

Due to the non-negligible dynamics of the pitch systems, the actuator dynamics is modeled by a first or second-order delay system. For example, the first-order system is

$$\dot{\beta} = -\frac{1}{\tau} \beta + \frac{1}{\tau} \beta_d, \quad (58)$$

where β and β_d denote the actual and demanded pitch angle and τ denotes the delay time constant. Without tower and blade dynamics, the model is used as a benchmark model for fault detection and isolation (FDI) and fault tolerant control (FTC) in [64].

High-order model for controller verification: An open access simulation code FAST based on an high-order aeroelastic wind turbine model is provided by NREL (National Renewable Energy Laboratory) [39] with a reference turbine [40]. The FAST (Fatigue, Aerodynamics, Structures, and Turbulence) code is a comprehensive aeroelastic simulator capable of predicting the extreme and fatigue loads of two- and three-bladed horizontal-axis wind turbines.

The FAST model employs a combined modal and multibody dynamics formulation. The model for three-bladed turbines relates nine rigid bodies (earth, support platform, base plate, nacelle, armature, gears, hub, tail, and structure furling with the rotor) and five flexible bodies (tower, three blades, and drive shaft) summing up to 24 degrees of freedom.

Problem description: The main purpose of wind turbine control is to capture as much energy as possible while at the same time ensuring wind turbine safety and power quality standards. Although these objectives are closely related, they might conflict with each other if handled separately. Therefore, the control objective is to find a well-balanced method that yields a compromise between all objectives.

Energy capture: Extract as much energy as possible from the wind, taking into consideration some restrictions such as rated speed, rated power and cut-out wind speed, etc.

Mechanical loads: Minimize the reduction of the system's lifetime by preventing the system from excessive dynamic mechanical loads; hence ensure the wind turbine safety.

Power quality: The cost of energy is affected by the power quality. Poor power quality causes an increase in the cost of energy. Thus, to reduce the cost, the generated power is conditioned to comply with the required interconnection standards.

To achieve these objectives, the rotor speed and generator torque should not exceed upper bounds.

Assessment criteria: The control performance is assessed for two operating ranges: The partial and the full load range. In the partial load range the rotor speed is regulated to obtain optimum energy efficiency. The deviation from the optimum energy output will be evaluated by $J_{\text{RMSE}_{\text{Ref}}}$ (19). In the full load range the requirement change to a set-point controller to limit the energy production even with increasing wind speed and keep also the mechanical loads and pitch activity to a minimum. Here, the wind speed acts as a disturbance on the controller feedback loop thus the effect of the wind speed variation on the output is measured by $J_{\text{MSE}_{\text{Dst}}}$ (28). The pitch control effort in the full load range is measured by J_{peak_u} (22) and J_{ISU} (23).

To assess the relevant mechanical loads a few numbers of wind turbine specific performance metrics are used: First, for assessment of occurred extreme loads the maximum values of tower base moment, blade-root bending moments, and low-speed shaft torque in the drive train are measured during a step-gust simulation. Second, for assessment of the reduction of fatigue loads the damage

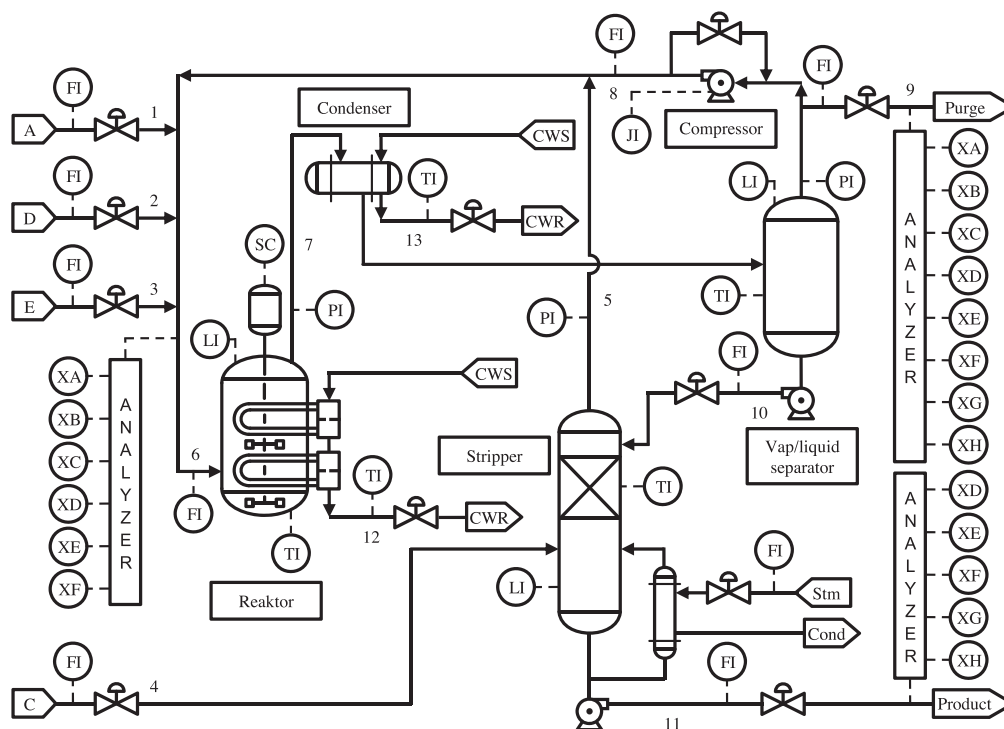


Fig. 13. Flowchart of Tennessee Eastman Process [51].

equivalent load range (DEL)⁵ of the tower base moment, blade-root bending moments, and low-speed shaft torque are calculated by normal operating conditions. That is, the turbine is subjected to a stochastic wind field with given mean wind speeds and turbulence intensities.

Examples of reported use: In [90], a gain scheduling controller design using a differential evolution optimization algorithm is presented. Here, the control-oriented model (55)–(58) without tower dynamics is used for controller verification. In [26], a fault-tolerant control concept for wind turbines using a Takagi-Sugeno sliding-mode observer is presented. The performance of the fault diagnosis and fault-tolerant control scheme is tested in simulations with the aero-elastic code FAST for the reference plant [40], a 5 MW three-bladed pitch-controlled wind turbine.

The presented benchmark received also attention in the conventional control community. In [78], a nonlinear model predictive controller (MPC) for wind turbines, and in [45], a combined feedback feedforward control using state-constrained MPC have been verified with the aero-elastic code. The control-oriented model is used in [9] for a linear parameter-varying control design (LPV).

3.13. Tennessee Eastman process control problem

Introduction: In the early 1990s, the company Eastman Chemicals, USA, contributed the Tennessee Eastman control problem [20]. It bases on an existing medium-size chemical process in industry. The description was modified due to business secrets. The plant is a nonlinear, instable, multi-variable process. The original benchmark was defined as process control problem. However, also other uses such as for fault diagnostics are reported.

Process description: Fig. 13 shows a flowchart of the process. The plant is continuously operated. Two products (G, H) are

produced from four gaseous reactants (A, C, D, E). An inert (B) is also present and a byproduct (F) occurs.

Products and byproduct are liquid. Hence, in total, 8 chemical species are involved in the process. The chemical reactions are irreversible and exothermic. The process is composed of five interacting major units: a continuously-stirred reactor, a condenser, a vapor-liquid separator and a stripper for the product stream as well as a centrifugal compressor for the recycle stream. The vapor and reaction liquid equilibrium equations are strongly nonlinear. The reactor dynamics are instable. Both products leave the plant in a single stream and are separated in a downstream distillation system that is not part of the benchmark problem. The process has 12 controllable inputs (flow rates, valve positions, drive speed) and 41 measured quantities (flow rates, levels, pressures, temperatures, power, concentrations). The original model has 50 states. Six modes of process operation are defined with the first mode (50/50 mass ratio of the two product streams) being the base case. A first-principles model and simulator (with integration step size of 1 sec.) is available as FORTRAN code and a simplified version as Matlab code from a website maintained by Prof. Lawrence Ricker [73].

Problem description: Six operational modes are specified that differ in ratio and absolute value of the product streams. The control objective is disturbance rejection, i.e. keeping some process quantities in given limits, minimal deviation of product rate and quality in case of disturbances as well as a quick recovery to nominal operation after disturbances or product rate changes.

Assessment criteria: The control performance is assessed for several step-type changes of reference values and disturbances. Amplitude and frequency of the variation of product rate and product composition are of particular interest. Movement of valves in feed streams should be minimized as they have a back effect on other units that feed the plant. Intentionally, no mathematical performance measures for control strategies were provided as issues such as sensor-fault tolerance, understandability by operators, hardware implementation etc. should also be considered in the assessment.

⁵ The damage-equivalent load range is calculated from the measured load signals and based on the relation between the load cycles equal to 1 sec and the rainflow load spectrum.

Table 11

Results for recursive model evaluation of PWA and TS throttle model for training and test data set.

Model	Data set	Criteria			Number of parameters	
		J_{MAE} in °	J_{RMSE} in °	J_{NRMSE} in °	Partitioning	Local models
PWA	Train	3.83	1.45	0.96	21	24
	Test	3.92	1.03	0.94		
TS	Train	4.47	1.42	0.91	16	24
	Test	3.74	1.06	0.95		

Examples of reported use: The benchmark primarily received attention in the conventional process control community; papers were in particular published in the “Control Engineering Practice” Journal, the “Journal of Process Control” and the “Computers and Chemical Engineering Journal”. Recently, also applications have been reported in the Soft Computing community. In [22], a hierarchical neural-network-based fault diagnosis method is tested with data generated from the Tennessee-Eastman process simulator. The proposed method involves fuzzy-c-means clustering and multi-layer perceptron networks. Diagnostic performance is assessed by the overall percentage of correct diagnosis and by the time required until the correct diagnosis is available after fault occurrence. In [52], a method for multi-PCA and ANFIS-based fault diagnosis is presented and demonstrated. Diagnostic performance is assessed by the missed detection rate, false alarm rate and fault-specific recognition rate. In [101], an adaptive, indirect neural network control approach is proposed as multivariable control scheme and tested against the Tennessee-Eastman process simulator. Disturbances rejection is assessed by the variance of the controlled variables. Secondly the number of disturbance scenarios that cause plant shutdown are computed. Set-point change performance is assessed by the required transition time. In [99], a recurrent/dynamical neural network is used to predict the compositions of species mixtures instead of using on-line gas chromatographs. The predictions are used to improve conventional PI control and for model-predictive control. Model performance is assessed by J_{RMSE} on training and validation data sets.

4. Conclusions and recommendations

A wider engagement in testing and demonstrating novel methods on benchmark problems is a rewarding undertaking for the individual researcher and for the community: Well-defined identification and control problems can be solved with moderate efforts while permitting to compare own results with results from other subject matter experts. Several well established benchmark problems ranging from single-input single-output problems to entire plants have been collected and presented in a uniform way in this paper. Many problems have not intentionally been published as benchmark problems with all experimental conditions and assessment criteria been well defined, but developed into such. Therefore many original publications do not provide the complete information required for a benchmark problem to permit validation, reproducibility and comparability. This translates into the same data used for identification or the same reference and disturbance signals for control and a set of accepted common assessment criteria. On the contrary, it is important that the benchmark adopters adhere to the details of the benchmark. For example, sometimes a continuous-time system is sampled with different sample-time. In case alteration of the original problem is preferred by an adopter it is recommended to provide also the results for both the original as well as the altered problem. Often it remains unspecified whether prediction errors refer to one-step-ahead or recursive model evaluation, so it is asked for precision here. The following two examples illustrate the authors' view on how results for the identification

benchmark in Section 3.4 and the control benchmark in Section 3.12 could be reported.

4.1. Throttle benchmark

Two models were identified for the throttle benchmark from Section 3.4: A piecewise affine and a Takagi-Sugeno model that have the same general structure: Both use $c=8$ local models. The features used for partitioning are $(y(k-1) - y(k-2))$ and $u(k-1)$ and the local models are

$$\hat{y}(k) = a_{1i} \cdot y(k-1) + a_{2i} \cdot y(k-2) + b_i \cdot u(k-1) + a_{0i}.$$

The major difference is that the PWA model uses crisp polyhedral partitions, but the TS model a soft partitioning with membership functions of fuzzy-c-means type. The assessment criteria determined for recursive model evaluation are recorded in Table 11. The corresponding frequency plots of the residuals on the test data set are shown in Fig. 14.

4.2. Wind turbine benchmark

Wind turbines are operated in different regimes depending on the wind speed conditions. In the nonlinear full-load region, the pitch angle is used as control input to reduce the aerodynamic lift force on the rotor blades and thereby to keep the rotor speed at its desired value.

For several operating points a linear LQR control design based on a linearized reduced-order model are combined to a PDC (parallel distributed compensation) controller in a Takagi-Sugeno (TS) structure. The obtained PDC controller is used for rotor speed control in

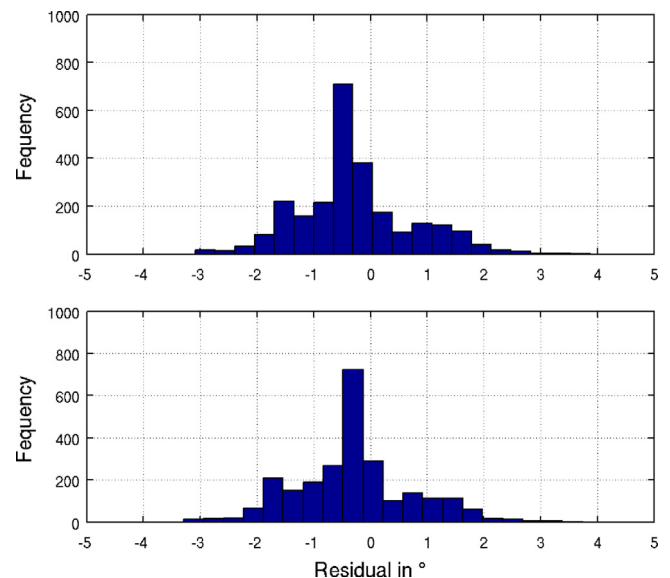


Fig. 14. Frequency plot of residuals from recursive model evaluation for PWA (top) and TS model (bottom) for test data set.

Table 12
Assessment criteria results of a PDC wind turbine controller.

$J_{\text{MSE}_{\text{DST}}}$	J_{peak_u}	J_{ISU}
$9.298 \cdot 10^{-4} \text{ (rad/s)}^2$	$3.608 \times 10^{-1} \text{ rad}$	2.316 rad^2

FAST simulations [26]. For controller verification $J_{\text{MSE}_{\text{DST}}}$, J_{peak_u} , and J_{ISU} were determined and are listed in Table 12.

Acknowledgements

The authors thank the anonymous reviewers for their constructive comments. In addition they are grateful to Axel Dürrbaum for assistance in \LaTeX typesetting and Salman Zaidi for the throttle modeling results.

References

- [1] J. Abonyi, B. Feil, Cluster analysis for data mining and system identification, Birkhäuser, Basel, 2007, Example 4.2.
- [2] A. Akhenak, M. Chadli, D. Maquin, J. Ragot, State estimation via multiple observer with unknown inputs: application to the three tank system, in: 5th IFAC Symposium on Fault Detection, Supervision and Safety for Technical Processes, Safeprocess'2003, Washington, USA, 2003 <http://hal.archives-ouvertes.fr/hal-00278202/en/>
- [3] S. Al-Assadi, Neural network-based model reference adaptive control for electronic throttle systems, in: Proceedings of SEA 2007 World Congress, Detroit, USA, 2007.
- [4] C. Anderson, W. Miller, A challenging set of control problems, in: Neural networks for control, MIT Press, Cambridge, MA, 1990, pp. 475–510, Appendix A.
- [5] C.W. Anderson, Learning to control an inverted pendulum using neural networks, IEEE Control Syst. Mag. 9 (1989) 31–37.
- [6] H. Aschemann, J. Ritzke, H. Schulte, Model-based nonlinear trajectory control of a drive chain with hydrostatic transmission, Proc. MMAR 16 (2009) 239–244.
- [7] M.H. Beale, M.T. Hagan, H.B. Demuth, Neural Network Toolbox: User's Guide, The Mathworks Inc., Natick, MA, 2013, Section A.
- [8] T. Bernd, M. Kleutges, A. Kroll, Nonlinear black box modelling: fuzzy systems versus neural networks, Neural Comput. Appl. 8 (1999) 151–162.
- [9] F.D. Bianchi, H. de Battista, R.J. Mantz, Wind Turbine Control Systems, Springer, London, 2007.
- [10] L. Blahová, J. Dvoran, Neuro-fuzzy control of the three tank system., in: 18th International Conference on Process Control, Tatranská Lomnica, Slovakia, 2011.
- [11] S. Blažič, I. Škrjanc, D. Matko, Globally stable direct fuzzy model reference adaptive control, Fuzzy Sets Syst. 139 (2003) 3–33.
- [12] X. Brun, S. Sesmat, D. Thomasset, S. Scavarda, A comparative study between two control laws of an electropneumatic actuator, in: European Control Conference ECC'99, Karlsruhe, Germany, 1999.
- [13] S. Cao, N. Rees, G. Feng, Analysis and design of a class of complex control systems. Part I: Fuzzy modelling and identification, Automatica 33 (1997) 1017–1028.
- [14] K. Dadhe, R. Gesthuisen, S. Engell, Estimating the prediction uncertainty of dynamic neural network process models, in: Proceedings of 7th IFAC Symposium on Dynamics and Control of Process Systems, 2004, pp. 829–840.
- [15] B. de Moor, DalSy: Database for the identification of systems, 2012 <http://homes.esat.kuleuven.be/smc/daisy/>
- [16] DELVE (2013). <http://www.cs.toronto.edu/delve/data/datasets.html>
- [17] Dixon, R. (2012). <http://www.staff.lboro.ac.uk/elrd2/>
- [18] R. Dixon, A. Pike, Alstom benchmark challenge II on Gasifier control, IEE Proc. Control Theor. Appl. 153 (2006) 254–261.
- [19] H.T. Do, K.K. Ahn, Velocity control of a secondary controlled closed-loop hydrostatic transmission system using an adaptive fuzzy sliding mode controller, J. Mech. Sci. Technol. 27 (2013) 875–884.
- [20] J. Downs, E. Vogel, A plant-wide industrial process control problem, Comput. Chem. Eng. 17 (1993) 245–255.
- [21] M.O. Efe, E. Abadoglu, O. Kaynak, A novel analysis and design of neural network assisted nonlinear control for a bioreactor, Int. J. Robust Nonlinear Control 9 (1999) 799–815.
- [22] R. Eslamloueyan, Designing a hierarchical neural network based on fuzzy clustering for fault diagnosis of the Tennessee Eastman process, Appl. Soft Comput. 11 (2011) 1407–1415.
- [23] A. Farag, H. Werner, Structure selection and tuning of multi-variable PID controllers for an Industrial Benchmark problem, IEE Proc. Control Theor. Appl. 153 (2006) 262–267.
- [24] L. Feldkamp, G. Puskorius, Neural network control of an unstable process, in: Proceedings of the 36th Midwest Symposium on Circuits and Systems, 1993.
- [25] R. Gasch, J. Tuele, Wind Power Plants, Springer, London, 2012.
- [26] S. Georg, H. Schulte, Actuator fault diagnosis and fault-tolerant control of wind turbines using a Takagi-Sugeno sliding mode observer, in: 2nd International Conference on Control and Fault-Tolerant Systems, SysTol 13, Nice, France, 2013.
- [27] S. Georg, H. Schulte, H. Aschemann, Control-oriented modelling of wind turbines using a Takagi-Sugeno model structure, in: IEEE International Conference on Fuzzy Systems, Brisbane, Australia, 2012, pp. 1–8.
- [28] P. Gerland, H. Schulte, A. Kroll, Probability-based global state detection of complex technical systems and application to mobile working machines, in: European Control Conference 2009 (ECC), Budapest, Hungary, 2009, pp. 1269–1274.
- [29] GMA Benchmarking. (2014). <http://www.rst.e-technik.tu-dortmund.de/cms/de/Veranstaltungen/GMA-Fachausschuss/Benchmark/index.html>
- [30] D. Gorinevsky, Sampled-data indirect adaptive control of bioreactor using affine radial basis function network architecture, Trans. ASME J. Dyn. Syst. Control 119 (1997) 94–97.
- [31] K. Graichen, V. Hagenmeyer, M. Zeitz, Design of adaptive feedforward control under input constraints for a benchmark CSTR based on a BVP solver, Comput. Chem. Eng. 33 (2009) 473–483.
- [32] B. Heiming, J. Lunze, Definition of the three-tank benchmark problem for controller reconfiguration, in: Proceedings of the European Control Conference, ECC'99, Karlsruhe, Germany, 1999.
- [33] F. Hoffmann, R. Mikut, A. Kroll, M. Reischl, O. Nelles, H. Schulte, T. Bertram, Computational intelligence, State-of-the-Art Methoden und Benchmarkprobleme., in: Proceedings of 22 Workshop Computational Intelligence, Dortmund, Germany, 2012, pp. 1–42.
- [34] J. Huang, G. Ji, Y. Zhu, P. van den Bosch, Identification of multi-model LPV models with two scheduling variables, J. Process Control 22 (2012) 1198–1208.
- [35] IFAC Technical Committee 1.1 (2014). <http://www.tc.ifac-control.org/1/1/DataRepository>
- [36] S. Iplikci, A support vector machine based control application to the experimental three-tank system, ISA Trans. 49 (2010) 376–386.
- [37] S. Iplikci, Support vector machine based neuro-fuzzy control of nonlinear systems, Neurocomputing 73 (2010) 2097–2107.
- [38] B. Jamali, H. Jazayeri-Rad, Application of adaptive local linear model tree for nonlinear identification of heat recovery steam generator system based on experimental data, in: 4th UKSim European Symposium on Computer Modeling and Simulation, 2010, pp. 16–20.
- [39] J. Jonkman, Nwtc design codes (fast by jason jonkman), 2013 <http://wind.nrel.gov/designcodes/simulators/fast/>
- [40] J. Jonkman, S. Butterfield, W. Musial, G. Scott, Definition of a 5-mw reference wind turbine for offshore systems development, 2009, nrel/tp-500-38060, technical report.
- [41] A.Q. Khan, S.X. Ding, C.I. Chihai, M. Abid, W. Chen, Robust fault detection in nonlinear systems: a three-tank benchmark application, in: Conference on Control and Fault Tolerant Systems, Nice, France, 2010, pp. 347–352.
- [42] K.-U. Klatt, S. Engell, Rührkesselreaktor mit Parallel- und Folgereaktion, in: Nichtlineare Regelung, VDI, Düsseldorf, 1993, pp. 101–111.
- [43] K.-U. Klatt, S. Engell, Gain-scheduling trajectory control of a continuous stirred tank reactor, Comput. Chem. Eng. 22 (1998) 491–502.
- [44] K.-U. Klatt, S. Engell, A. Kremling, F. Allgöwer, Testbeispiel: Rührkesselreaktor mit Parallel- und Folgereaktion, in: Entwurf nichtlinearer Regelungen, Oldenbourg, Munich, 1995, pp. 425–432.
- [45] A. Körber, R. King, Combined feedback feedforward control of wind turbines using state-constrained model predictive control, IEEE Trans. Control Syst. Technol. 21 (2013) 1117–1128.
- [46] D. Krokavec, A. Filasova, Stabilizing fuzzy output control for a class of nonlinear systems advances in fuzzy systems, Adv. Fuzzy Syst. (2013), <http://dx.doi.org/10.1155/2013/294971>.
- [47] A. Kroll, Computational Intelligence - Eine Einführung in Probleme, Methoden und technische Anwendungen, Oldenbourg, Munich, 2013 <http://www.oldenbourg-verlag.de/wissenschaftsverlag/computational-intelligence/9783486709766>
- [48] A. Kugi, K. Schlacher, H. Aitzetmüller, G. Hirmann, Modeling and simulation of a hydrostatic transmission with variable-displacement pump, Math. Comput. Simul. 53 (2000) 409–414.
- [49] M. Kvasnica, M. Herceg, L. Čirka, M. Fikar, Model predictive control of a CSTR: A hybrid modeling approach, Chem. Pap. 64 (2010) 301–309, <http://dx.doi.org/10.2478/s11696-010-0008-8>.
- [50] H. Kwakernaak, R. Sivan, Linear Optimal Control Systems, Wiley, New York, 1972.
- [51] T. Larsson, K. Hestetun, E. Hovland, S. Skogestad, Self-optimizing control of a large-scale plant: the Tennessee Eastman process, Ind. Eng. Chem. Res. 40 (2001) 4889–4901.
- [52] C. Lau, K. Ghosh, M. Hussain, C. Che Hassan, Fault diagnosis of Tennessee Eastman process with multi-scale PCA and ANFIS, Chemom. Intell. Lab. Syst. 120 (2013) 1–14.
- [53] J. Li, K. Tanaka, Intelligent control for pneumatic servo system, JSME Int. J. 46 (2001) 699–704.
- [54] W.L. Luyben, Process Modeling, Simulation and Control for Chemical Engineers, McGraw-Hill, New York, 1990.
- [55] I. Markovky, J. Willems, S.V. Huffel, B. de Moor, R. Pintelon, Application of structured total least squares for system identification and model reduction, IEEE Trans. Automat. Control 50 (2005) 1490–1500.
- [56] Mathworks, Fuzzy Logic Toolbox: User's Guide, The Mathworks Inc., Natick, MA, 2013.
- [57] Mathworks, Statistics Toolbox: User's Guide, The Mathworks Inc., Natick, MA, 2013, Section A.

- [58] L.F. Mendonça, J.M.C. Sousa, J.M.G.S. da Costa, Fault accommodation of an experimental three tank system using fuzzy predictive control, in: *IEEE International Conference on Fuzzy Systems, FUZZ-IEEE '08*, Seoul, Korea, 2008, pp. 1619–1625 <http://dblp.uni-trier.de/db/conf/fuzzIEEE/fuzzIEEE2008.html#MendoncaSC08>
- [59] S. Molov, R. Babuska, J. Abonyi, H. Verbruggen, Effective optimization for fuzzy model predictive control, *IEEE Trans. Fuzzy Syst.* 12 (2004) 661–675.
- [60] K. Narendra, K. Parthasarathy, Identification and control of dynamical systems using neural networks, *IEEE Trans. Neural Netw.* 1 (1990) 4–27.
- [61] O. Nelles, *Nonlinear System Identification*, Springer, Berlin, 2001.
- [62] NIST, Nist nonlinear regression reference datasets, 2013 http://www.itl.nist.gov/div898/strd/nls/nls_main.shtml
- [63] NIST, Nist statistical reference datasets (strd) description, 2013 <http://www.nist.gov/itl/sed/gsg/strd.cfm>
- [64] P.F. Odgaard, J. Stoustrup, M. Kinnaert, Fault tolerant control of wind turbines a benchmark model, in: *Proceedings of the 7th IFAC Symposium on Fault Detection, Supervision and Safety of Technical Processes*, Barcelona, Spain, 2009.
- [65] J.C. Ossyra, *Control Concepts for Vehicle Drive Line to Reduce Fuel Consumption*, VDI Verlag, Düsseldorf, 2005, Fortschritt-Berichte VDI Reihe 12, Nr. 598.
- [66] S. Papadakis, J. Theodoris, A GA-based fuzzy modeling approach for generating TSK models, *Fuzzy Sets Syst.* 131 (2002) 121–152.
- [67] S. Postalciglu, K. Erkan, Soft computing and signal processing based active fault tolerant control for benchmark process, *J. Neural Comput. Appl.* 18 (2009) 77–85.
- [68] G. Puskorius, L. Feldkamp, Neurocontrol of nonlinear dynamical systems with Kalman filter trained recurrent networks, *IEEE Trans. Neural Netw.* 5 (1994) 279–297.
- [69] Z. Ren, A. Kroll, M. Sofsky, F. Laubenstein, On methods for automated modeling of dynamic systems with friction and their application to electro-mechanical throttles, in: *49th IEEE Conference on Decision and Control*, Atlanta, GA, USA, 2010, pp. 7637–7642.
- [70] Z. Ren, A. Kroll, M. Sofsky, F. Laubenstein, On identification of piecewise-affine models for systems with friction and its application to electro-mechanical throttles, in: *16th IFAC Symposium on System Identification (Sysid 2012)*, Brüssel, Elsevier Ltd., Belgium, 2012, pp. 1395–1400.
- [71] Z. Ren, A. Kroll, M. Sofsky, F. Laubenstein, On physical and data-driven modeling of systems with friction: methods and application to automotive throttles, *at-Automatisierungstechnik* 61 (2013) 155–171 (in German).
- [72] E. Richard, S. Scavarda, Comparison between linear and nonlinear control of an electropneumatic servodrive, *J. Dyn. Syst. Meas. Control* 118 (1996) 245–252.
- [73] N. Ricker, *Tennessee Eastman Challenge Archive*, 1993 <http://depts.washington.edu/control/LARRY/TE/download.html>
- [74] J.K. Roberge, *The Mechanical Seal*. Bachelor's thesis, Massachusetts Institute of Technology, 1960.
- [75] K. Salahshoor, M. Hamzehnejad, A novel online affine model identification of multivariable processes using adaptive neuro-fuzzy networks, *Chem. Eng. Res. Des.* 88 (2010) 155–169.
- [76] B. Sanandaji, K. Salahshoor, A. Fatehi, Multivariable GA-based identification of TS fuzzy models: MIMO distillation column model case study, in: *IEEE International Fuzzy Systems Conference*, London, 2007.
- [77] J.F. Schaefer, R.H. Cannon, On the control of unstable mechanical systems, in: *Proceedings of the third Automatic and Remote Control* 3, 1966, pp. 12–24.
- [78] D. Schlupf, D.J. Schlupf, M. Kühn, Nonlinear model predictive control of wind turbines using LIDAR, *Wind Energy* (2012), <http://dx.doi.org/10.1002/we.1533>.
- [79] H. Schulte, Control-oriented modeling of hydrostatic transmissions using Takagi-Sugeno fuzzy systems, in: *IEEE International Conference on Fuzzy Systems, FUZZ-IEEE '07*, London, UK, 2007.
- [80] H. Schulte, G. Gerland, Observer design using T-S fuzzy systems for pressure estimation in hydrostatic transmissions, in: *International Conference on Intelligent Systems Design and Applications, ISDA '09*, Pisa, Italy, 2009, pp. 779–784.
- [81] H. Schulte, H. Hahn, Fuzzy state feedback gain scheduling control of servopneumatic actuators, *Control Eng. Pract.* 12 (2004) 639–650.
- [82] G. Serra, C. Bottura, An IV-QR algorithm for neuro-fuzzy multivariable online identification, *IEEE Trans. Fuzzy Syst.* 15 (2007) 200–210.
- [83] R.A. Seyab, Y. Cao, Nonlinear model predictive control for the Alstom gasifier, *J. Process Control* 16 (2006) 795–808.
- [84] M.-C. Shih, N.-L. Luor, Self-Tuning Neural Fuzzy Control the position of pneumatic cylinder under vertical load, in: *6th International Symposium on Fluid Control Measurement and Visualization (FLUCOME 2000)*, Sherbrooke, QC, Canada, 2000.
- [85] A. Simm, G. Liu, Improving the performance of the ALSTOM baseline controller using multiobjective optimisation, *IEE Proc. Control Theor. Appl.* 153 (2006) 286–292.
- [86] R. Sivakumar, K.S. Manic, V. Nerthiga, R. Akila, K. Balu, Application of fuzzy model predictive control in multivariable control of distillation column, *Int. J. Chem. Eng. Appl.* 1 (2010) 38–42.
- [87] S. Skogestad, Dynamics and control of distillation columns: a tutorial introduction, *Chem. Eng. Res. Des.* 75 (1997) 539–562.
- [88] S. Skogestad, *Binary distillation column model "A"*, 2014 http://www.nt.ntnu.no/users/skoge/book/matlab_m/cola/cola.html
- [89] M. Smaoui, X. Brun, D. Thomasset, Systematic control of an electropneumatic system: Integrator backstepping and sliding mode control, *Trans. Control Syst. Technol.* 14 (2006) 905–913.
- [90] S.A. Taher, M. Farshadnia, M.R. Mozdianfard, Optimal gain scheduling controller design of a pitch-controlled VS-WECS using DE optimization algorithm, *Appl. Soft Comput.* 13 (2013) 2215–2223.
- [91] UCI, 2013, UC Irvine Machine Learning Repository, 2013 <http://archive.ics.uci.edu/ml/>
- [92] L. Ungar, A bioreactor benchmark for adaptive network-based process control, in: W.M.R. Sutton, P. Werbos (Eds.), *Neural Networks for Control* chapter 16, MIT Press, Cambridge, MA, 1990, pp. 387–402.
- [93] T. Utz, V. Hagenmeyer, B. Mahn, Comparative evaluation for nonlinear model predictive and flatness-based two-degree-of-freedom control design in view of industrial application, *J. Process Control* 17 (2007) 129–141.
- [94] M. Vasak, L. Mladenovic, N. Peric, Clustering-based identification of a piecewise affine electronic throttle model, in: *31st Annual Conference IEEE Industrial Electronics Society*, 2005, pp. 177–182.
- [95] H.O. Wang, K. Tanaka, M.F. Griffin, An approach to fuzzy control of nonlinear systems: Stability and design issues, *IEEE Trans. Fuzzy Syst.* 4 (1996) 14–23.
- [96] X. Wang, K. Wu, J. Lu, W. Xiang, Nonlinear identification of Alstom gasifier based on Wiener model, in: *International Conference on Sustainable Power Generation*, Nanjing, PR China, 2009.
- [97] K. Weischedel, T. McAvoy, Feasibility of decoupling in conventionally controlled distillation columns, *Ind. Eng. Chem. Fund.* 19 (1980) 379–384.
- [98] WEKA (2013), <http://www.cs.waikato.ac.nz/ml/weka/datasets.html>
- [99] T. Yeh, M. Huang, C.T. Huang, Estimate of process compositions and plantwide control from multiple secondary measurements using artificial neural networks, *Comput. Chem. Eng.* 27 (2003) 55–72.
- [100] J. Yi, N. Yubazaki, K. Hirota, Upswing and stabilization control of inverted pendulum system based on the sirms dynamically connected fuzzy inference model, *Fuzzy Sets Syst.* 122 (2001) 139–152.
- [101] S. Zerkaoui, F. Druaux, E. Leclercq, D. Lefebvre, Indirect neural control for plant-wide systems: application to the Tennessee Eastman Challenge Process, *Comput. Chem. Eng.* 34 (2010) 232–243.